Aquaculture 600 (2025) 742243

Contents lists available at ScienceDirect

Aquaculture

journal homepage: www.elsevier.com/locate/aquaculture

Potential role of Mc3r and Mc4r in ovarian metabolism and development in female red crucian carp (*Carassius auratus* red var.)

Faxian Yu [a,1], Lu Huang [a,1], Xinxin Yu [a,1], Shuxin Zhang [a], Shengnan Li [a], Rong Zhou [a], Wenjing Tao [b], Lanying Yang [b], Min Tao [a,*], Qizhi Liu [a,*], Shaojun Liu [a,*]

[a] State Key Laboratory of Developmental Biology of Freshwater Fish, College of Life Sciences, Hunan Normal University, Changsha 410081, Hunan, China
[b] Key Laboratory of Freshwater Fish Reproduction and Development (Ministry of Education), Key Laboratory of Aquatic Science of Chongqing, Southwest University, Chongqing 400715, China

ARTICLE INFO

Keywords:
Red crucian carp
Mc3r
Mc4r
Reproduction
Omics analysis

ABSTRACT

Melanocortin-3 and -4 receptors (MC3R and MC4R) play a crucial role in regulating multiple physiological processes in mammals, such as reproduction. In this study, we aimed to determine the function of Mc3r and Mc4r in regulating reproduction, particularly ovarian development, in red crucian carp *(Carassius auratus* red var.). Situ hybridization showed *mc3r* and *mc4r* signals in areas of the pituitary gland and ovary linked to reproductive hormone secretion, suggesting these receptors regulate reproduction in RCC. Ovarian histology revealed that *mc3r* and *mc4r* mutations disrupted the contact between the follicular cell layer and the zona radiata compared to WT, with this disruption more common in *mc4r*$^{+/-}$ fish. KEGG enrichment analysis further showed that differentially expressed genes (DEGs) were enriched in pathways involved in steroid hormone biosynthesis, oocyte meiosis, progesterone-mediated oocyte maturation, and GnRH signaling, all related to reproduction. Additionally, several DEGs associated with ovarian development, follicle formation, oocyte maturation, and ovulation were found in these pathways. The results of qRT-PCR showed that *mc3r* and *mc4r* mutations reduced the expression of key reproductive genes in the hypothalamic-pituitary-gonadal axis. The integrated analysis of the liver transcriptome and metabolome found that DEGs and differential metabolites in WT and mutated fish were enriched in pathways related to steroid hormone biosynthesis, growth, and lipid accumulation. In conclusion, these results will aid foundation for investigating the molecular mechanisms of Mc3r/Mc4r-meidated reproduction in fish.

1. Introduction

The melanocortin agonists are post-translational products of proopiomelanocortin (POMC), comprising of α- melanocyte-stimulating hormone (MSH), β-MSH, γ- MSH, and adrenocorticotropic hormone (ACTH) (Dores and Lecaude, 2005; Gantz and Fong, 2003). Throughout the evolution of teleost, POMC paralogues have undergone subfunctionalization in both their expression patterns and peptide domains (De Souza et al., 2005). The melanocortin agonists exert distinct physiological functions via acting on the five melanocortin receptors (MCRs, MC1R-MC5R) to regulate the melanocortin system (Cortés et al., 2014; Gantz and Fong, 2003). MCRs belong to rhodopsin-like Family A G-protein-coupled receptors (GPCRs) with even transmembrane domains, which play essential roles in regulating multiple physiological functions (Gantz and Fong, 2003). Among the MCRs, MC3R and MC4R are highly expressed in the central nervous system (CNS) in mammals, with important roles in the regulation of feeding, growth, and energy expenditure (Chen et al., 2000; Balthasar et al., 2005; Huszar et al., 1997; Zhang et al., 2005).

MC3R and MC4R also play a role in regulating the secretion of reproductive hormones, sexual function, and reproduction in mammals (Martin and MacIntyre, 2004). In humans, MC3R affects the timing of sexual maturation, and the mutations in *MC3R* show a delayed onset of puberty (Duckett et al., 2023; Lam et al., 2021; Zheng et al., 2023). The female mice lacking *Mc3r* exhibit uniquely reproductive phenotypes (Bedenbaugh et al., 2023). Similar to the *MC3R* mutation, the *MC4R* mutation is associated with alterations in the timing of puberty onset, polycystic ovary syndrome, and hypogonadotropic hypogonadism in

* Corresponding authors.
E-mail addresses: minmindiu@126.com (M. Tao), lqz@hunnu.edu.cn (Q. Liu), lsj@hunnu.edu.cn (S. Liu).
[1] These authors have contributed equally to this work.

https://doi.org/10.1016/j.aquaculture.2025.742243
Received 23 May 2024; Received in revised form 26 December 2024; Accepted 29 January 2025
Available online 2 February 2025

humans (Aldhoon Hainerová et al., 2011; Batarfi et al., 2019; Doulla et al., 2014). Additionally, MC4R can affect the secretions of luteinizing hormone (LH) and prolactin (PRL) by promoting leptin-MCR signaling in rats (Watanobe et al., 1999; Watanobe et al., 2001). Moreover, *Mc4r*-deficient mice show decreased cystic follicles, corpora lutea, and ovulation rate (Sandrock et al., 2009).

Numerous studies have also highlighted the critical roles of teleost Mc3r and Mc4r in regulating feeding (Aspiras et al., 2015; Schjolden et al., 2009), growth (Huang et al., 2024; Ji et al., 2021), lipid accumulation (Du et al., 2023), and energy expenditure (Yang et al., 2019; Zhang et al., 2012), as well as reproduction. In common carp, *mc3r* with high expression in the brain activate the cAMP and MAPK signaling pathways and inhibit TNF-α-induced NF-κB signaling (Du et al., 2023). Culter Mc3r has high constitutive activity in the cAMP pathway, while reduced expression of *mc3r*, *mc4r*, and *pomc* is more involved in adults (Ji et al., 2021). The mRNA of fish *mc3r* is also found in the ovary, which is linked to reproductive hormone secretion, suggesting a role in fish reproduction (Du et al., 2023; Huang et al., 2024; Ji et al., 2021; Yu et al., 2022). However, specific data on Mc3r's role in fish reproduction is still lacking.

In teleosts, Mc4r affects reproductive hormone secretion and the onset of puberty. Mc4r influences the expression of genes related to reproduction, such as gonadotropin-releasing hormone (*gnrh*), follicle-stimulating hormone beta (*fshβ*), luteinizing hormone beta (*lhβ*), Cytochrome P450 11 (*cyp11*), Cytochrome P450 19 (cyp19), 3β-Hydroxysteroid Dehydrogenase (*3β-hsd*), and Steroidogenic Acute Regulatory (*star*) (Jiang et al., 2017; Zhang et al., 2020). Additionally, *mc4r* expression increases with ovarian development and is prominently located in ovarian follicles (Zhang et al., 2020). Mc4r also plays a role in puberty regulation in medaka (*Oryzias latipes*) (Liu et al., 2019), swordtail (*Xiphophorus nigrensis*) (Lampert et al., 2010), and platyfish (*Xiphophorus maculatus*) (Volff et al., 2013).

The hypothalamic-pituitary-gonadal (HPG) axis plays an important role in regulating reproduction in mammals (Yang et al., 2017). The hypothalamus secretes the gonadotropin-releasing hormone (GnRH) in a pulsatile manner (Herbison, 2018). Then, the GnRH acts on the pituitary to produce follicle-stimulating hormone (FSH) and luteinizing hormone (LH) (Golyszny et al., 2022). These hormones circulate to the ovary to produce estrogens, which facilitate the maturation of gametes, ovulation, and secretion of progesterone (Knobil, 1990). Manfredi-Lozano et al. found that the leptin-melanocortin-kisspeptin system is located upstream of GnRH pathway, and the MCRs (MC3R and MC4R) are located upstream of kisspeptin and downstream of leptin and ghrelin, indicating MC3R and MC4R are involved in regulating reproduction via HPG axis (Manfredi-Lozano et al., 2016). Similar results also reported in teleosts (Jiang et al., 2017; Liu et al., 2020).

The red crucian carp (*Carassius auratus* red var., RCC), which belongs to Cypriniformes, Cyprinidae, Carassius, is an economically important fish widely distributed in the rivers and lakes throughout Asia. Because the red crucian carp is one of the important fish species in aquaculture. It has a fast growth rate and strong reproductive capacity. It is highly adaptable and can tolerate various environmental conditions. In laboratory settings, it is relatively easy to breed and rear. Under suitable conditions, it reaches sexual maturity in 6 to 8 months. Moreover, it shares significant biological similarities with other fish species, and its biological and genetic studies are well-established. Therefore, the red crucian carp is chosen as a research subject. In this study, we explored the localization of *mc3r* and *mc4r* in the pituitary gland and ovary, investigated the ovarian histology and the expression of key genes related to regulation of reproduction in WT, *mc3r*$^{+/-}$, and *mc4r*$^{+/-}$, and further analyzed the transcriptome of ovary among WT vs. *mc3r*$^{+/-}$, WT vs. *mc4r*$^{+/-}$, and *mc3r*$^{+/-}$ vs. *mc4r*$^{+/-}$ and further integrated analysis of the liver transcriptome and the metabolome among WT vs. *mc3r*$^{+/-}$, WT vs. *mc4r*$^{+/-}$, and *mc3r*$^{+/-}$ vs. *mc4r*$^{+/-}$. These data laid the foundation for exploring the reproductive regulation of Mc3r and Mc4r in fish.

2. Materials and methods

2.1. Animal and ethics statement

The RCC with mutated *mc3r* (*mc3r*$^{+/-}$) and *mc4r* (*mc4r*$^{+/-}$) had been obtained by the CRISPR/Cas9 system in the previous study (Huang et al., 2024). The wild type (WT), *mc3r*$^{+/-}$, and *mc4r*$^{+/-}$ RCC were farmed in the Engineering Research Center of Polyploid Fish Reproduction and Breeding of the Ministry of Education at Hunan Normal University. A total of 54 six-month-old fish (18 per group: WT, 10.28 ± 2.18 g; *mc3r*$^{+/-}$, 10.38 ± 2.27 g; *mc4r*$^{+/-}$, 16.80 ± 4.68 g) were randomly selected. Each group was placed in three separate parallel tanks for rearing (6 fish per tank). During the experiment, water quality parameters were closely monitored and maintained at stable levels: water temperature was controlled at 26.0 ± 1.0 °C, pH was maintained at 8.0 ± 0.5, dissolved oxygen levels were kept between 6.0 and 7.0 mg/L and the light regime was set to a 12-h light/12-h dark cycle. Commercial diets were fed twice a day, at 09:00 and 17:00. After 12 days of feeding, all fish were anesthetized with tricaine methane sulfonate (MS222, Sangon Biotech, China) and sampled immediately. All animal experiments were approved by the Animal Care Committee of Hunan Normal University and carried out following the Guide for the Care and Use of Laboratory Animals.

2.2. In situ hybridization

Primers used for in situ hybridization (ISH) and the steps of ISH were identical as described previously (Huang et al., 2024). In brief, the pituitary gland and ovary were fixed in 4 % paraformaldehyde (PFA, Sangon) for a night, dehydrated with sucrose solutions, embedded in Tissue-Tek O.C.T. Compound® (Sakura, USA), and then cut into 20-μm-thick sections for ISH. ISH was performed in an RNAase-free environment. Firstly, the sections were treated with 1 × PBST, proteinase K, 4 % PFA, and prehybridization solution. Next, the treated sections were incubated in hybridization solution for 16 h. Then, the hybridized sections were incubated with AP-conjugated anti-DIG antibody after a series of washes. Finally, the treated sections were stained with NBT/BCIP stock solution (Roche, Germany), and light microscopy (Olympus, Japan) was used to detect the hybridization signals.

2.3. Hematoxylin-eosin (HE)

Ovary was collected from 6-month-old WT, *mc3r*$^{+/-}$, and *mc4r*$^{+/-}$ fish and fixed in 4 % PFA at 4 °C for 24 h. Subsequently, these tissues were dehydrated with a graded series of alcohol (70 %, 80 %, 90 %, 95 %, and 100 %), immersed with xylene (alcohol: xylene = 1:1), embedded in paraffin wax, and sliced into 5 μm. After that, these sliced sections were stained with hematoxylin and eosin according to the instructions. Finally, the stained sections were examined under the Olympus light microscope (Tokyo, Japan).

2.4. Transcriptome sequencing

Two fish ovarian tissues were randomly sampled from each replicate (total 6 per group) were placed in 2 mL enzyme-free centrifuge tubes containing RNAlater, and then transferred to −80 °C for storage for transcriptome sequencing. The steps of transcriptome sequencing were performed as described previously (Huang et al., 2024). In brief, extraction of total RNA of samples, construction of cDNA libraries, sequence of cDNA libraries using Illumina HiSeq™ sequencing platform, and then data analysis. Quality control of the sequenced data was performed using fastp software. Sequence comparison of Clean Reads to the reference genome was performed using HISAT2 software. The results of genome sequence comparison were analyzed by IGV software. Differential expression analysis between samples was performed using DESeq2 to obtain sets of differentially expressed genes between the two

biological conditions. The genes with |log2Fold Change| ≥1 and false discovery rate (FDR) < 0.05 were defined as differentially expressed genes (DEGs). Transcriptome sequencing results were mapped and analyzed on the Metware Biotechnology cloud platform (https://cloud.metware.cn/#/home). Blast2 GO was used for GO functional analysis of DEGs and GO function notes were classified into three categories: biological process (BP), cellular component (CC), and molecular function (MF). Moreover, we found several DEGs associated with ovarian development in these pathways and a cluster map was drawn using Metware Cloud. The raw reads were submitted to NCBI under accession PRJNA1107086. The reference genome used in this study is GCF_003368295.1_ASM336829v1_genomic.fna, download link: https://www.ncbi. nlm.nih.gov/datasets/genome/?taxon=7957.

2.5. Untargeted metabolomics analysis

Liver tissues ($n = 6$) of 6-month-old WT, *mc3r*$^{+/-}$ and *mc4r*$^{+/-}$ fish were thawed on ice, then 20 ± 1 mg of each thawed tissue were added to 1.5 mL Eppendorf (EP) tube and homogenized for 30s followed by centrifugation at 3000 r/min for 30s. Next, 400 μL of extraction solution (methanol: water = 4:1) was added to the EP tube, and the mixture was vortexed for 5 min at 1500 rpm before standing on ice for 15 min. After centrifuging at 12,000 rpm for 10 min at 4 °C, 300 μL of the supernatant was transferred into a sterile EP tube. This was then incubated for 30 min at 20 °C. Following this incubation, the supernatant was subjected to a second centrifugation at 12,000 rpm for 3 min at 4 °C. The final supernatant was collected for liquid chromatography-tandem mass spectrometry (LC-MS/MS) analysis.

The LC-MS/MS analysis was conducted using the 1290 Infinity LC and the Waters ACQUITY UPLC HSS T3 C18 column (2.1 × 100 mm, 1.8 um) with a flow rate of 0.4 mL/min, the column temperature was set to 40 °C, and the injection volume was 2 μL. The mobile phases consisted of solvent A (0.1 % formic acid in water) and solvent B (0.1 % formic acid in acetonitrile). The elution gradient was as follows: 0-11 min (95 % A and 5 % B), 11–12 min (10 % A and 90 % B), 12–12.1 min (10 % A and 90 % B), 12.1–14 min (95 % A and 5 % B).

The mass spectrometric data was collected via QTOF/MS-6545 (Agilent, USA) equipped with electrospray ionization (ESI) operating in positive and negative modes. The parameters of the ion spray voltage in positive mode (POS) and negative mode (NEG) were 2500 V (ESI+) and 1500 V (ESI-), respectively. The parameters of gas flow, fragmetor, gas temperature, sheath temperature, sheath flow, and nebulizer were 8 L/min, 135 V, 325 °C, 325 °C, 11 L/min, and 40 V, respectively.

The raw data obtained from LC-MS/MS were converted into MzXML files using ProteoWizard, and XCMS software was used to extract the peak intensities, peak match, and correct the retention time. SIMCA-p software V14.1 was used for multivariate statistical analysis, including principal component analysis (PCA) and orthogonal partial least-squares discrimination analysis (OPLS-DA) models. The metabolites with importance for the project (VIP) > 1 and $p < 0.05$ were defined as differential metabolites (DMs). The functions and enrichment analysis of DMs were performed using the KEGG database.

2.6. Quantitative reverse transcriftion PCR

Total RNA was extracted from the ovary of six-month-old WT, *mc3r*$^{+/-}$, and *mc4r*$^{+/-}$ fish with Trizol™ reagent (Invitrogen). The first-strand cDNA was generated using PrimeScript RT reagent kit with gDNA Eraser (TaKaRa). AlleleID 6 was used to design the specific primers for quantitative reverse transcription PCR (qRT-PCR) according to the partial cDNA fragment of the coding region of the published target genes (Table S1). The amplification parameters and procedures of qRT-PCR were performed according to the previous reports (Huang et al., 2024; Huang et al., 2021; Ji et al., 2021; Tao et al., 2020). The relative expression levels of these genes were normalized by the $2^{-\Delta\Delta Ct}$ method (Livak and Schmittgen, 2001) and the *β-actin* was used as the reference gene.

2.7. Integration of transcriptomic and metabolomics

Transcriptomic data were published in the previous study (Huang et al., 2024). Pearson correlation coefficients of transcriptomics and metabolomics were calculated via an R package (Hmisc). All DEGs and DMs were mapped into the KEGG database to understand the connections between DEGs and DMs.

2.8. Statistical analysis

GraphPad Prism 7.0 software (GraphPad Software, San Diego, CA, USA) was used to perform statistical analyses, including the calculation of means and standard error of the mean (SEM), and to generate graphical representations of the data. All data were presented as the mean ± SEM. Significant differences in gene expression between the mutated and WT fish were determined using a student's *t*-test. The $p < 0.05$ was considered statistically significant.

3. Results

3.1. The localization of RCC mc3r and mc4r in pituitary gland and ovary

ISH was used to determine the localization of *mc3r* and *mc4r* mRNA in the RCC pituitary gland and ovary (Fig. 1) (Clemence Girardet et al., 2018). Results showed that both the *mc3r* and *mc4r* mRNA were widely expressed in pituitary, especially with strong signals in NH and marginal zones of the PI and slightly weak signals in the RPD and PPD (Fig. 1A and B). Furthermore, the *mc4r* signals appeared stronger than the *mc3r* signals (Fig. 1A and B). There were no positive signals in the negative control (Fig. 1C).

To understand the role of Mc3r and Mc4r in ovarian, we detected the localization of these two genes in the ovary at different developmental stages. We found that *mc3r*-labeled (Fig. 1D) and *mc4r*-labeled (Fig. 1E) cells were detected at the nucleus, cytoplasm of oocytes; the signals in the nucleus appeared stronger than in the cytoplasm. In addition, *mc3r* (Fig. 1G) and *mc4r* (Fig. 1H) mRNAs were observed at follicular cells, zona radiata, cortical alveoli, and yolk granules. Similarly, the signals of *mc4r* in the ovary were stronger than those in *mc3r*. No positive signals were observed in the negative control (Fig. 1F and I).

3.2. Ovarian histology

The ovarian development of 6-month-old WT, *mc3r*$^{+/-}$, and *mc4r*$^{+/-}$ fish showed that most oocytes were at phases II and III and some oocytes at phase IV (Fig. 2A-C). Interestingly, the *mc3r*$^{+/-}$ (Fig. 2B1) and *mc4r*$^{+/-}$ (Fig. 2C1) fish showed loss of contact between the follicular cell layer and the zona radiata compared with the WT (Fig. 2A1). Moreover, the phenomenon in the oocyte of *mc4r*$^{+/-}$ fish was more common than in *mc3r*$^{+/-}$ fish (Fig. 2B1—C1) (Table 1).

3.3. Untargeted metabolic profile

To understand the effects of Mc3r and Mc4r on the metabolism, we conducted a metabolomic analysis of liver samples of WT, *mc3r*$^{+/-}$, and *mc4r*$^{+/-}$ by LC-MS/MS. The result of PCA showed significant separation in WT, *mc3r*$^{+/-}$, and *mc4r*$^{+/-}$, indicating metabolites had significant changes in the three groups (Fig. S1A). Based on the screening criteria (VIP > 1 and $p < 0.05$), a total of 724 DMs were screened in the three groups. Compared to the WT, 254 DMs (221 up-regulated and 33 down-regulated) and 318 DMs (120 up-regulated and 198 down-regulated) were identified in *mc3r*$^{+/-}$ and *mc4r*$^{+/-}$, respectively. Compared to the *mc3r*$^{+/-}$, 471 DMs (76 up-regulated and 395 down-regulated) were identified in *mc4r*$^{+/-}$ (Fig. S1B—D). Furthermore, hierarchical clustering was used for the distribution of DMs in each group, and the

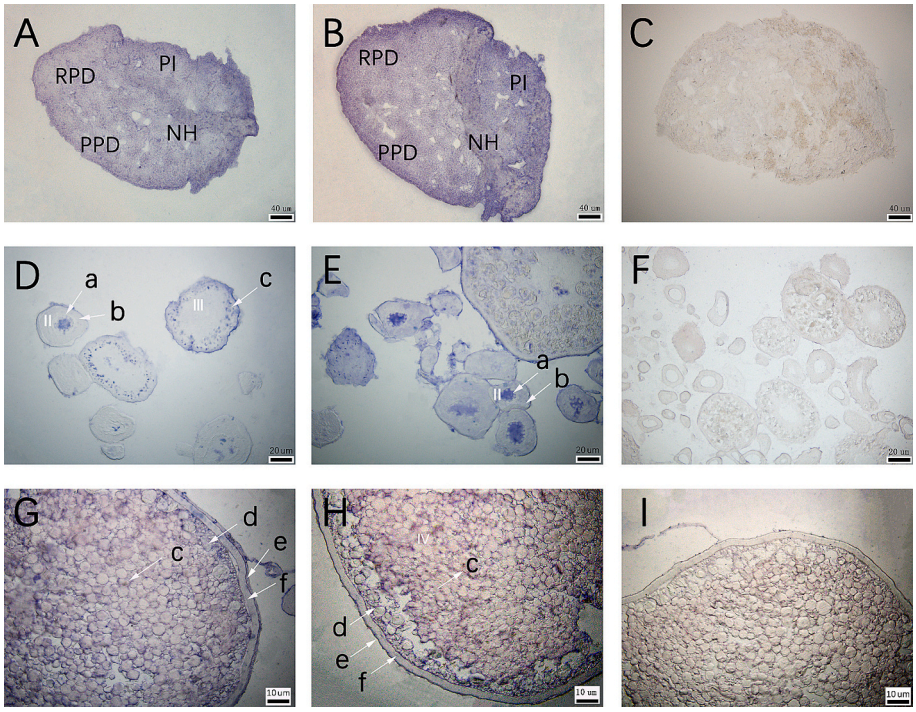

Fig. 1. Localization of *mc3r* and *mc4r* in RCC pituitary gland and ovary.
(A)Localization of *mc3r* in RCC pituitary gland. (B) Localization of *mc4r* in RCC pituitary gland. (C) Negative control of RCC pituitary gland. (D) Localization of *mc3r* in RCC ovary (E) Localization of *mc4r* in RCC ovary. (F) Negative control of RCC ovary. (G) Localization of *mc3r* in RCC ovary. (H) Localization of *mc4r* in RCC ovary. (I)Negative control of RCC ovary.
Neurohypophysis (NH); Pars intermedia (PI); Proximal pars distalis (PPD); Rostral pars distalis (RPD); II, III, and IV indicate oocytes in phases I, II, III, and IV, respectively; a represents nucleus of oocytes; b represents cytoplasm of oocytes; c represents yolk granules; d represents cortical alveoli; f represents zona radiata; e represents follicular cells. Scale bar: 40 μm (A, B, and C), 20 μm (D, E, and F), 10 μm (G, H, and I).

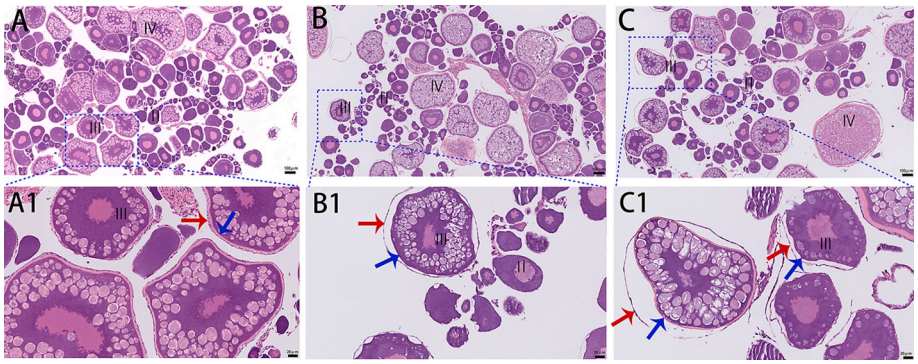

Fig. 2. Ovarian histology of WT, $mc3r^{+/-}$, and $mc4r^{+/-}$.
(A, A1) Ovarian histology of WT. (B, B1) Ovarian histology of $mc3r^{+/-}$. (C, C1) Ovarian histology of $mc4r^{+/-}$. The red arrows indicate the follicular cell layer; The blue arrows denote the zona radiata. Scale bar: 100 μm (A, B, and C), 20 μm (A1, B1, and C1). (For interpretation of the references to color in this figure legend, the reader is referred to the web version of this article.)

Table 1
Separation of the follicular cell layer and the zona radiata in WT, $mc3r^{+/-}$, and $mc4r^{+/-}$.

Group	Separation ratio (%)
WT	0.004 ± 0.0069^{a}
$mc3r^{+/-}$	0.311 ± 0.0048^{b}
$mc4r^{+/-}$	0.148 ± 0.0223^{c}

Values with different superscripts in the same column are significantly different ($p < 0.05$). Data are shown as the mean ± SEM ($n = 3$).

hierarchical clustering heatmap was divided into 2 clusters among the groups. Biological replicates in each group clustered together, indicating great biological reproducibility and reliability of the data (Fig. S1E-G).

The KEGG pathway enrichment analysis of WT VS. $mc3r^{+/-}$ demonstrated that DMs were mainly enriched in tryptophan metabolism, metabolic pathways, biosynthesis of cofactors, aminoacyl-tRNA biosynthesis, D-Amino acid metabolism, fructose and mannose metabolism, and ABC transporters (Fig. 3A). In WT VS. $mc4r^{+/-}$, the DMs were mainly enriched in sphingolipid metabolism, pyruvate metabolism, drug metabolism-cytochrome P450, cAMP signaling pathway, tryptophan metabolism, retinol metabolism, Glycosaminoglycan biosynthesis-heparan sulfate/heparin, and sphingolipid signaling pathway (Fig. 3B). In $mc3r^{+/-}$ VS. $mc4r^{+/-}$, the DMs were mainly

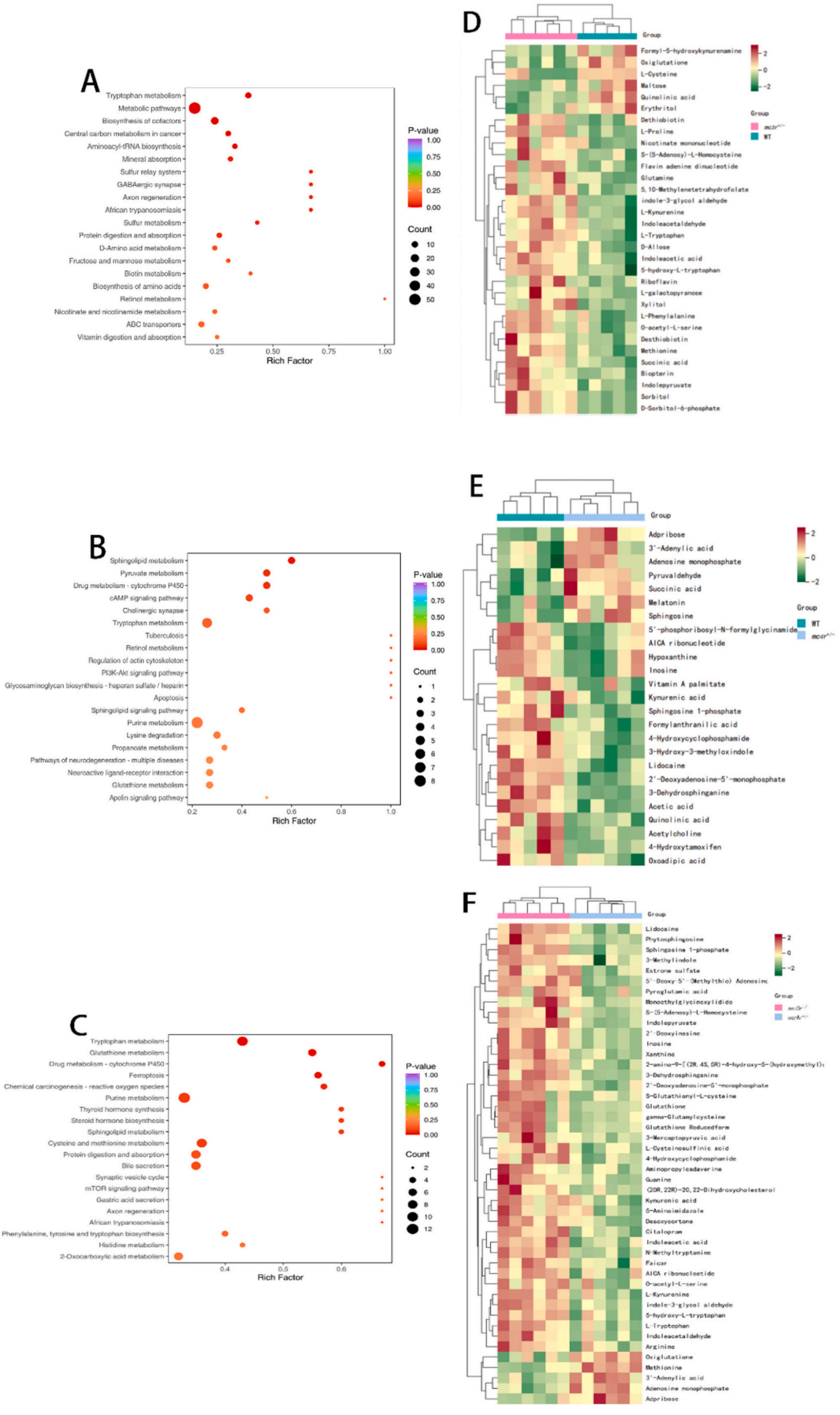

(caption on next page)

Fig. 3. KEGG enrichment analysis and hierarchical clustering heatmap of DMs in the liver.
(A) KEGG enrichment analysis of the DMs in WT vs. *mc3r*$^{+/-}$. (B) KEGG enrichment analysis of the DMs in WT vs. *mc4r*$^{+/-}$. (C) KEGG enrichment analysis of the DMs in *mc3r*$^{+/-}$ vs. *mc4r*$^{+/-}$. (D) Hierarchical clustering heatmap of DMs in WT vs. *mc3r*$^{+/-}$. (E) Hierarchical clustering heatmap of DMs in WT vs. *mc4r*$^{+/-}$. (F) Hierarchical clustering heatmap of DMs in *mc3r*$^{+/-}$ vs. *mc4r*$^{+/-}$. In the KEGG enrichment analysis, the vertical coordinate represents the pathway, and the horizontal coordinate represents the Rich factor. The larger the Rich factor, the greater the degree of enrichment. The larger the dot, the greater the number of DMs enriched in the KEGG. The redder the color of the dot, the more significant the enrichment. In hierarchical clustering heatmap, the vertical coordinate represents the metabolite, and the horizontal coordinate represents the sample. Different colors represent different relative contents obtained after standardized treatment (red represents high content, green represents low content).

enriched in tryptophan metabolism, glutathione metabolism, drug metabolism-cytochrome P450, purine metabolism, steroid hormone biosynthesis, sphingolipid metabolism, cysteine and methionine metabolism, and mTOR signaling pathway (Fig. 3C).

Hierarchical clustering was performed to visualize those DMs that are enriched in the above pathways. Hierarchical clustering heatmap showed that formyl-5-hydroxykynurenamine, oxiglutatione, l-cysteine, maltose, quinolinic acid, and erythritol had lower expression, while the other 26 DMs had higher expression in *mc3r*$^{+/-}$ compared to WT (Fig. 3D). The adpribose, 3′-Adenylic acid, adenosine monophosphate, pyruvaldehyde, succinic acid, melatonin, and sphingosine showed increased levels, but the other DMs showed decreased levels in *mc4r*$^{+/-}$ compared to WT (Fig. 3E). In *mc4r*$^{+/-}$, the levels of oxiglutatione, methionine, 3′-Adenylic acid, adenosine monophosphate, and adpribose were higher, but remaining DMs were lower than in *mc3r*$^{+/-}$ (Fig. 3F).

3.4. Transcriptome analysis and qRT-PCR verification

Transcriptome analysis of WT, *mc3r*$^{+/-}$, and *mc4r*$^{+/-}$ in the ovary was performed to examine the role of Mc3r and Mc4r in regulating reproduction, especially ovarian development.

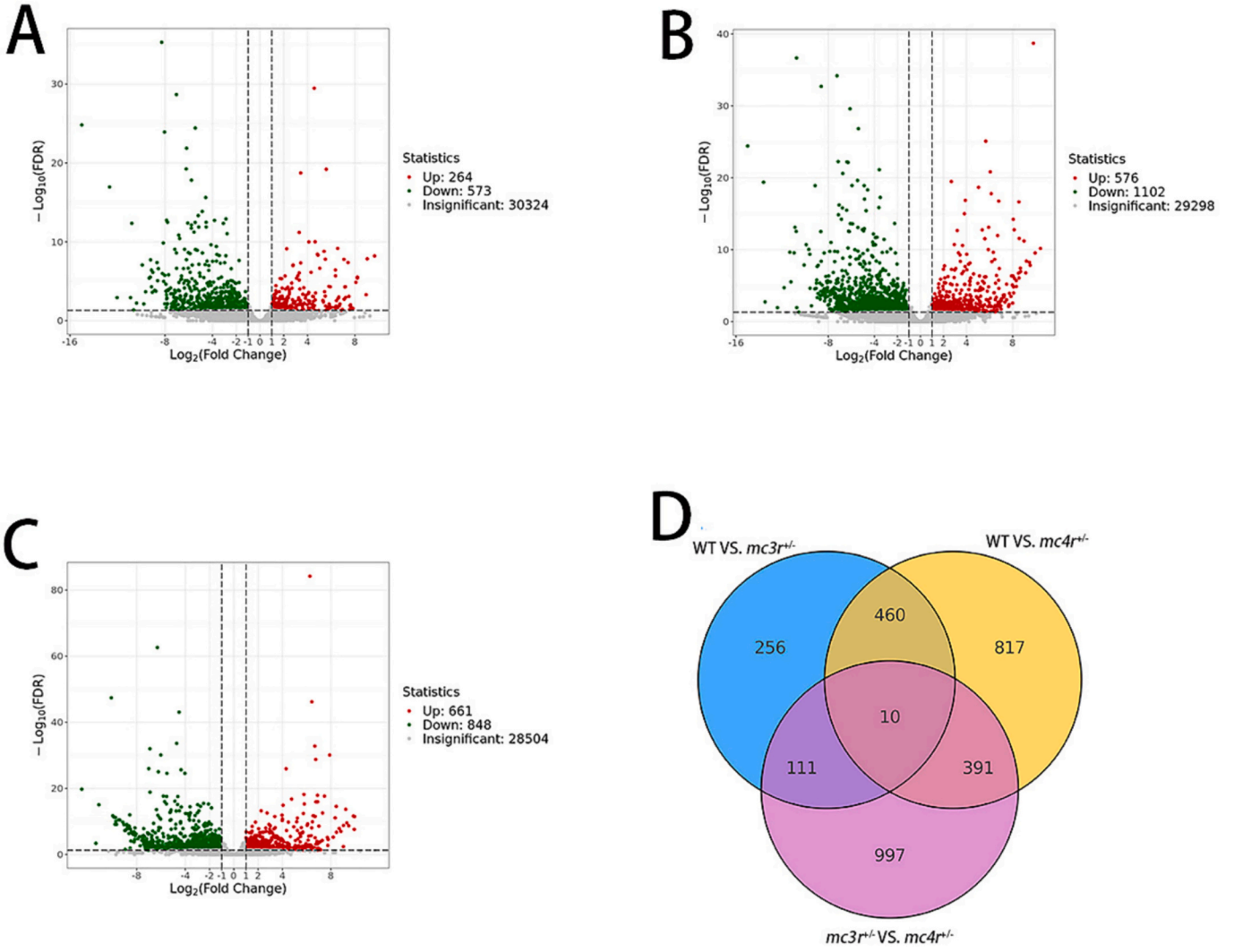

Fig. 4. Volcano map and Venn diagram of EDGs in the ovary.
(A) Volcano map of DEGs in WT vs. *mc3r*$^{+/-}$. (B) Volcano map of DEGs in WT vs. *mc4r*$^{+/-}$. (C) Volcano map of DEGs in *mc3r*$^{+/-}$ vs. *mc4r*$^{+/-}$. (D) Venn diagram of EDGs in WT vs. *mc3r*$^{+/-}$, WT vs. *mc4r*$^{+/-}$, and *mc3r*$^{+/-}$ vs. *mc4r*$^{+/-}$. In the Volcano map, significantly up-regulated and down-regulated genes are highlighted in red and green, respectively, and insignificant genes are shown in gray. In the Venn diagram, the non-overlapping region represents the unique DEGs for the differential group and the overlapping region represents the shared DEGs for the differential group. (For interpretation of the references to color in this figure legend, the reader is referred to the web version of this article.)

3.4.1. Analysis of DEGs

The result showed that a total of 837 DEGs were screened in WT vs. *mc3r*$^{+/-}$, among which 264 DEGs were up-regulated and 573 DEGs were down-regulated (Fig. 4A). In WT vs. *mc4r*$^{+/-}$, a total of 1678 DEGs were identified, including 576 up-regulated DEGs and 1102 down-regulated DEGs (Fig. 4B). In addition, there were 1509 DEGs in *mc3r*$^{+/-}$ vs. *mc4r*$^{+/-}$, among which 661 DEGs exhibited up-regulation and 848 DEGs exhibited down-regulation (Fig. 4C). Venn diagram indicated that the numbers of overlap DEGs in the three comparison groups were 10 (Fig. 4D).

3.4.2. Go enrichment analysis of DEGs

GO enrichment analysis of DEGs was performed and the top 20 enrichment items were shown in Fig. S2.

In WT vs. *mc3r*$^{+/-}$ (Fig. S2A), there were 25 GO terms for BP including cellular process (GO:0009987) with 617 DEGs, metabolic process (GO:0008152) with 443 DEGs, reproduction (GO:0000003) with 68 DEGs, and reproductive process (GO:0022414) with 68 DEGs. There were 2 GO terms for CC including protein-containing complex (GO:0032991) with 202 DEGs and cellular anatomical entity (GO:0110165) with 701 DEGs. There were 16 GO terms for MF including binding (GO:0005488) with 506 DEGs, catalytic activity (GO:0003824) with 256 DEGs, molecular function regulator (GO:0098772) with 105 DEGs, and transcription regulator activity (GO:0140110) with 4 DEGs. GO enrichment analysis showed that the serine-type endopeptidase inhibitor activity, endopeptidase inhibitor activity, and endopeptidase regulator activity were the most enriched (Fig. S2D).

In WT vs. *mc4r*$^{+/-}$ (Fig. S2B), there were 26 GO terms for BP including cellular process (GO:0009987) with 1158 DEGs, biological regulation (GO:0065007) with 813 DEGs, metabolic process (GO:0008152) with 812 DEGs, and reproduction (GO:0000003) with 110 DEGs. There were 2 GO terms for CC including protein-containing complex (GO:0032991) with 394 DEGs and cellular anatomical entity (GO:0110165) with 1366 DEGs. There were 16 GO terms for MF including binding (GO:0005488) with 976 DEGs, catalytic activity (GO:0003824) with 480 DEGs, molecular function regulator (GO:0098772) with 175 DEGs, and transcription regulator activity (GO:0140110) with 106 DEGs. GO enrichment analysis showed that the binding of sperm to zona pellucida, sperm-egg recognition, and single fertilization were the most enriched (Fig. S2E).

In *mc3r*$^{+/-}$ vs. *mc4r*$^{+/-}$ (Fig. S2C), there were 24 GO terms for BP including cellular process (GO:0009987) with 1077 DEGs, biological regulation (GO:0065007) with 746, metabolic process (GO:0008152) with 738 DEGs, and reproduction (GO:0000003) with 90 DEGs. There were 2 GO terms for CC including cellular anatomical entity (GO:0110165) with 1225 DEGs and protein-containing complex (GO:0032991) with 358 DEGs. There were 16 GO terms for MF including binding (GO:0005488) with 857 DEGs, catalytic activity (GO:0003824) with 426 DEGs, molecular function regulator (GO:0098772) with 148 DEGs, and transcription regulator activity (GO:0140110) with 91 DEGs. GO enrichment analysis showed that the binding of sperm to zona pellucida, cell-cell recognition, and sperm-egg recognition were the most enriched (Fig. S2F).

3.4.3. KEGG enrichment analysis of DEGs

To identify the biological functions of *mc3r* and *mc4r* in ovarian development, the DEGs of the three groups were mapped to the pathways in the KEGG database. KEGG enrichment analysis of WT vs. *mc3r*$^{+/-}$ indicated that 273 DEGs were enriched in 144 pathways and 13 pathways were significantly enriched ($p < 0.05$). In WT vs. *mc4r*$^{+/-}$, KEGG enrichment analysis showed that 516 DEGs were enriched in 155 pathways and 14 pathways were significantly enriched ($p < 0.05$). In *mc3r*$^{+/-}$ vs. *mc4r*$^{+/-}$, KEGG enrichment analysis revealed that 469 DEGs were enriched in 147 pathways and no pathway was significantly enriched ($p < 0.05$).

In addition, we found DEGs enriched in some pathways related to ovarian growth and development. In WT vs. *mc3r*$^{+/-}$, DEGs enriched in apoptosis, ribosome, glutathione metabolism, adipocytokine signaling pathway, PPAR signaling pathway, steroid hormone biosynthesis, MAPK signaling pathway, Wnt signaling pathway, oocyte meiosis, and p53 signaling pathway (Fig. 5A). In WT vs. *mc4r*$^{+/-}$, DEGs enriched in oocyte meiosis, progesterone-mediated oocyte maturation, TGF-beta signaling pathway, adipocytokine signaling pathway, metabolism of xenobiotics by cytochrome P450, p53 signaling pathway, steroid hormone biosynthesis, PPAR signaling pathway, Wnt signaling pathway, MAPK signaling pathway, insulin signaling pathway, GnRH signaling pathway, and steroid biosynthesis (Fig. 5B). In *mc3r*$^{+/-}$ vs. *mc4r*$^{+/-}$, DEGs enriched in spliceosome, apelin signaling pathway, oocyte meiosis, p53 signaling pathway, Wnt signaling pathway, mTOR signaling pathway, drug metabolism-cytochrome P450, MAPK signaling pathway, PPAR signaling pathway, progesterone-mediated oocyte maturation, FoxO signaling pathway, insulin signaling pathway, TGF-beta signaling pathway, and GnRH signaling pathway (Fig. 5C). Moreover, 22 key DEGs associated with reproduction and ovarian development were found in these pathways such as fibroblast growth factor 10 (*fgf10*), MA and mother against decapentaplegic (MAD)-related proteins 4 (*smad4*), MA and mother against decapentaplegic (MAD)-related proteins 6 (*smad6*), *Cyclin B1*, *Cyclin B2*, mitotic arrest deficient 2 like 2 (*ad2l2*), recombinant vang like protein 1 (*vangl1*), poly [ADP-ribose] polymerase 1 (*parp1*), salmon GnRH (*sGnRH*), DNA binding inhibitory factor (*id3*), glutathione reductase (*gsr*), hepatocyte growth factor (*hgf*), insulin like growth factor 1 receptor (*igf1r*), adiponectin receptor protein 1 (*adipor1*), calcium signaling activator calmodulin 1 (*calm1*), mini-chromosome maintenance protein 5 (*mcm5*), wingless-type MMTV integration site family (*wnt5a*), nucleoside diphosphate kinase 3 (*nme3*), tyrosine-protein phosphatase non-receptor type 11 (*ptpn11*), forkhead box protein M1 (*foxm1*), mitogen-activating protein kinase 1 (*mapk1*), and cullin-4B (*cul4b*) (Fig. 5D).

3.4.4. DEGs verification by qRT-PCR

To further verify the reliability of transcriptome data, 9 genes (f-box only protein 5 (*fbxo5*), proto-oncogene c-Fos (*fos*), glutathione reductase (*gsr*), phosphodiesterase 5A (*PDE5a*), serine/threonine-protein phosphatase 2 A catalytic subunit (*PP2 A-α*), serine/threonine-protein phosphatase 2 A 56 kDa regulatory subunit (*ppp2r5ea*), poly [ADP-ribose] polymerase 1 (*ppt1*), 60S ribosomal protein L35 (*rpl35*), and tumor protein p53 (*tp53)*) were selected to validate the expression patterns in the ovary by qRT-PCR. As shown in Fig. 6, the expression patterns of the 9 DEGs were consistent with the transcriptome data, indicating the reliability of transcriptome sequencing.

3.5. Integrated analysis of the transcriptome and the metabolome

To further investigate the mechanism of RCC *mc3r* and *mc4r* in glucolipid metabolism and reproductive regulation, the integrated analysis of the transcriptome and the metabolome was performed. In WT vs. *mc3r*$^{+/-}$, the DEGs and DMs were jointly enriched in 38 KEGG pathways, including metabolic pathways, biosynthesis of cofactors, and biosynthesis of amino acids (Fig. S3A). In WT vs. *mc4r*$^{+/-}$, the DEGs and DMs were jointly enriched in 58 KEGG pathways, including metabolic pathways, carbon metabolism, and biosynthesis of cofactors (Fig. S3B). In *mc3r*$^{+/-}$ vs. *mc4r*$^{+/-}$, the DEGs and DMs were jointly enriched in 46 KEGG pathways, including metabolic pathways, cysteine and methionine metabolism, and ferroptosis (Fig. S3C). We found some DEGs and DMs were jointly enriched in the 6 pathways including arginine and proline metabolism (DEGs: *proC*, *P4HA*, *ODC1*, and *GATM*. DMs: Proline and 4-Guanidinobutyric acid), alanine, aspartate and glutamate metabolism (DEGs: *AGXT*, *ASPA*, and *GLUL*. DMs: L-Glutamine, 2-Oxoglutaramate, succinate, and L-Asparagine), pyruvate metabolism (DEGs: *LDH*, *ACH1*, *ACS*, *PCK*, and *maeB*. DMs: methylglyoxal, succinate, and acetate), tyrosine metabolism (DEGs: *MIF*, *COMT*, and *DBH*. DMs: 3-Methoxy-4-hydroxymandelate), ferroptosis (DEGs: *SLC3A2*, *ACSL4*,

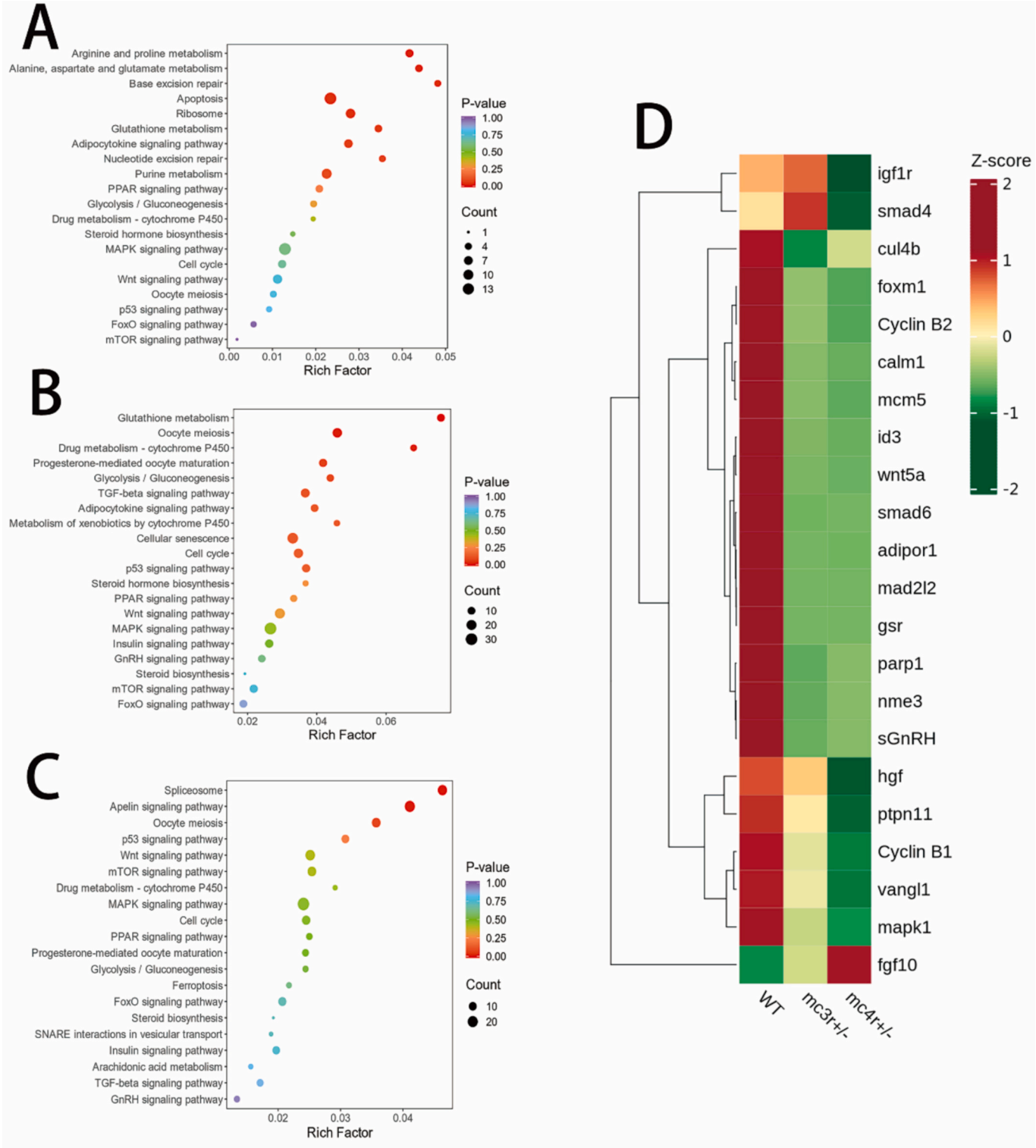

Fig. 5. KEGG enrichment analysis and hierarchical clustering heatmap of DEGs in the ovary.
(A) KEGG enrichment analysis of DEGs in WT vs. *mc3r*$^{+/-}$. (B) KEGG enrichment analysis of DEGs in WT vs. *mc4r*$^{+/-}$. (C) KEGG enrichment analysis of DEGs in *mc3r*$^{+/-}$ vs. *mc4r*$^{+/-}$. (D) Hierarchical clustering heatmap of EDGs in WT vs. *mc3r*$^{+/-}$, WT vs. *mc4r*$^{+/-}$, and *mc3r*$^{+/-}$ vs. *mc4r*$^{+/-}$. In the KEGG enrichment analysis, the vertical coordinate represents the pathway, and the horizontal coordinate represents the Rich factor. The larger the Rich factor, the greater the degree of enrichment. The larger the dot, the greater the number of DEGs enriched in the KEGG. The redder the color of the dot, the more significant the enrichment. In hierarchical clustering heatmap, the vertical coordinate represents the DEGs, and the horizontal coordinate represents the sample. Different colors represent different relative contents obtained after standardized treatment (red represents high content, green represents low content).

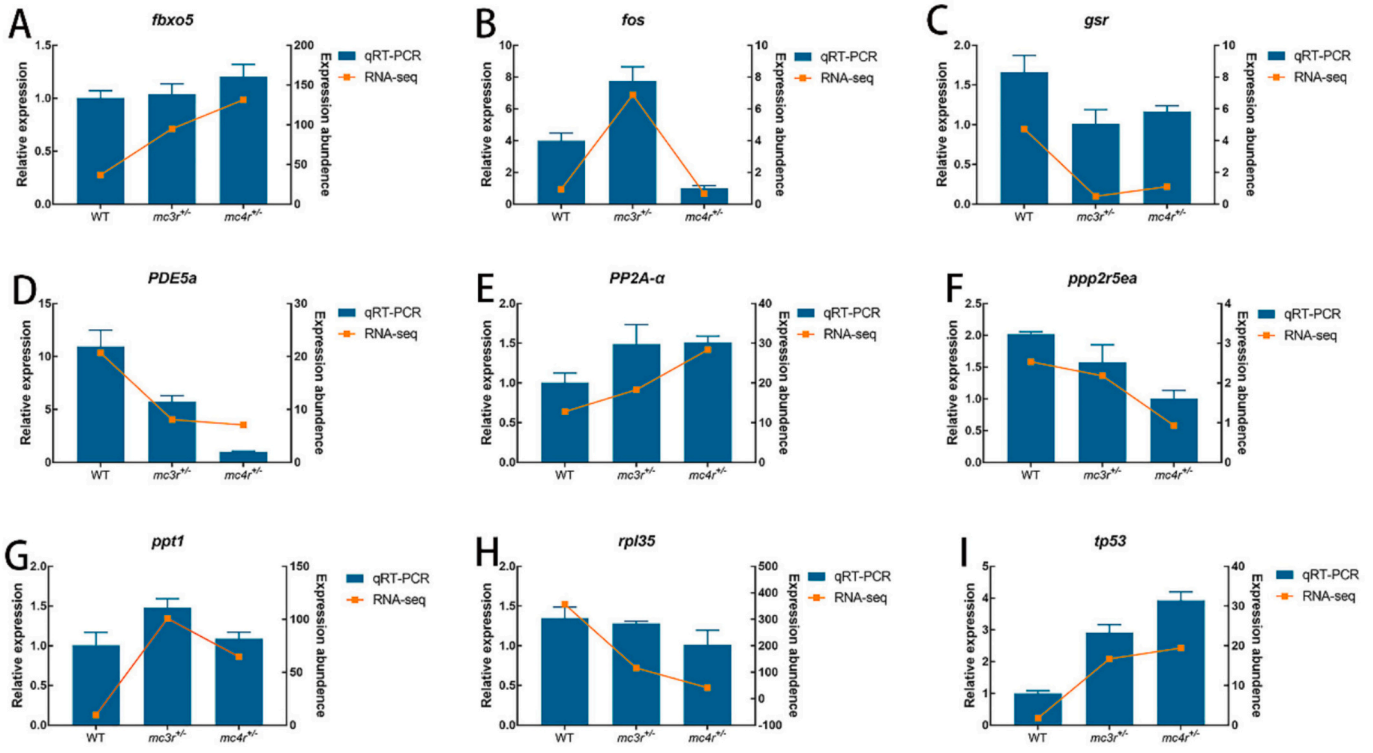

Fig. 6. qRT-PCR validation of the expression levels of the nine genes in WT, $mc3r^{+/-}$, and $mc4r^{+/-}$.
The relative expression of *fbxo5* (A), *fos* (B), *gsr* (C), *PDE5a* (D), *PP2 A-α* (E), *ppp2r5ea* (F), *ppt1* (G), *rpl35* (H), and *tp53* (I) in WT, $mc3r^{+/-}$, and $mc4r^{+/-}$. F-box only protein 5 (*fbxo5*); proto-oncogene c-Fos (*fos*); glutathione reductase (*gsr*); phosphodiesterase 5A (*PDE5a*); serine/threonine-protein phosphatase 2A catalytic subunit (*PP2A-α*); serine/threonine-protein phosphatase 2A 56 kDa regulatory subunit (*ppp2r5ea*); poly [ADP-ribose] polymerase 1 (*ppt1*); 60S ribosomal protein L35 (*rpl35*); tumor protein p53 (*tp53*). The *β-actin* was used as the internal control. The data were shown as the mean ± SEM ($n = 3$).

and *VDAC3*), and steroid hormone biosynthesis (DEGs: *UTG*, *HSD17B8*, and *SRD5A1*. DMs: estrone 3-sulfate) (Fig. 7).

3.6. Expression of key genes related to reproduction

To investigate the effect of *mc3r* and *mc4r* on reproduction, we examined the expression of key genes related to reproduction on the HPG axis in the ovary of WT, $mc3r^{+/-}$, and $mc4r^{+/-}$ fish by qRT-PCR (Fig. 8). The relative mRNA expression of kisspeptin-1 (*kiss1*) and steroidogenic acute regulatory protein (*star*) was significantly lower in $mc4r^{+/-}$ and slightly lower in $mc3r^{+/-}$ compared to the WT (Fig. 8 A, B). In addition, the *prolactin* expression was significantly lower in $mc4r^{+/-}$ than in WT, and the gene had a slightly reduced level in $mc3r^{+/-}$ compared to WT (Fig. 8 C). Regarding the other key genes such as G protein-coupled receptor a (*gpr54a*), G protein-coupled receptor b (*gpr54b*), *gnrh*, follicle-stimulating hormone beta *(fshβ)*, follicle-stimulating hormone receptor (*fshr*), luteinizing hormone beta *(lhβ)*, luteinizing hormone receptor (*lhr*), and cytochrome P450 19A1 (*cyp19a1a*), the mRNA expression levels of these genes were significantly lower in $mc3r^{+/-}$ and $mc4r^{+/-}$ compared to WT (Fig. 8 D—K), but there were no significant differences between $mc3r^{+/-}$ and $mc4r^{+/-}$. Additionally, the relative mRNA expression of *gpr54a*, *gnrh*, *fshr*, and *lhr* in $mc4r^{+/-}$ was slightly lower than those in $mc3r^{+/-}$, but the *gpr54b*, *fshβ*, and *lhβ* showed a reversed pattern between $mc3r^{+/-}$ and $mc4r^{+/-}$.

4. Discussion

To investigate the role of Mc3r and Mc4r in ovarian development, we examined the localization of these two genes expression in the pituitary gland and ovary of RCC using ISH. Our data showed that the mRNA levels of these two receptors were present in NH, PI, RPD, and PPD of pituitary gland (Fig. 1A, B). Previous studies have found that *gnrh*, *fshβ*, and *lhβ* mRNAs are also detected in these pituitary regions, where they stimulate gamete and ovary maturation (Gothilf et al., 1996; Guzmán et al., 2009; Pandolfi et al., 2006; Swanson et al., 2003). Furthermore, pituitary tissue treated with NDP-MSH (a non-selective agonist for Mc3r and Mc4r) and THIQ (a Mc4r selective agonist) showed increased expression of these genes in spotted scat (*Scatophagus argus*) and black rockfish (*Sebastes schlegelii*) (Jiang et al., 2017; Zhang et al., 2020). Furthermore, in the ovary, *mc4r*-labeled cells were observed in the nucleus, cytoplasm of oocytes, follicular cells, zona radiata, cortical alveoli, and yolk granules, consistent with previous study (Zhang et al., 2020). Similarly, *mc3r*-labeled cells were found in the same areas. Although specific reports on *mc3r* localization in teleost ovaries are lacking, several studies have shown that *mc3r* is highly expressed in the ovary (Huang et al., 2024; Ji et al., 2021; Navarro et al., 2022; Wu et al., 2022; Yu et al., 2022). Additionally, *mc4r* signals were detected stronger than *mc3r* signals in both the pituitary gland and ovary. Thus, our results suggest that both Mc3r and Mc4r might be involved in ovarian development, with Mc4r potentially playing a more significant role than Mc3r in regulating reproductive development.

To investigate the molecular mechanisms underlying histological and gene expression changes in mutated RCC, we conducted ovarian transcriptome sequencing. GO and KEGG analyses revealed that DEGs were enriched in pathways related to metabolism, reproduction, and ovarian development, including apoptosis, PPAR signaling, TGF-β/MAPK, insulin/FoxO signaling, and GnRH signaling— all of which play important roles in oocyte maturation, follicular development, and ovulation in mammals (Tilly, 1996; Hussein, 2005; Dupont et al., 2012; Strauss et al., 2014; Mantawy et al., 2019; Greenstein, 2005; Josefsberg Ben-Yehoshua et al., 2007; Edmonds et al., 2010; Liu et al., 2023b; Chen et al., 2019; Du et al., 2015). Genes like *CUL4B*, *Cyclin B1*, and *Cyclin B2* are essential for oocyte survival and maturation (Lin et al., 2016; Qiu et al., 2008; Yu, 2014), while ID3 influences oocyte quality and

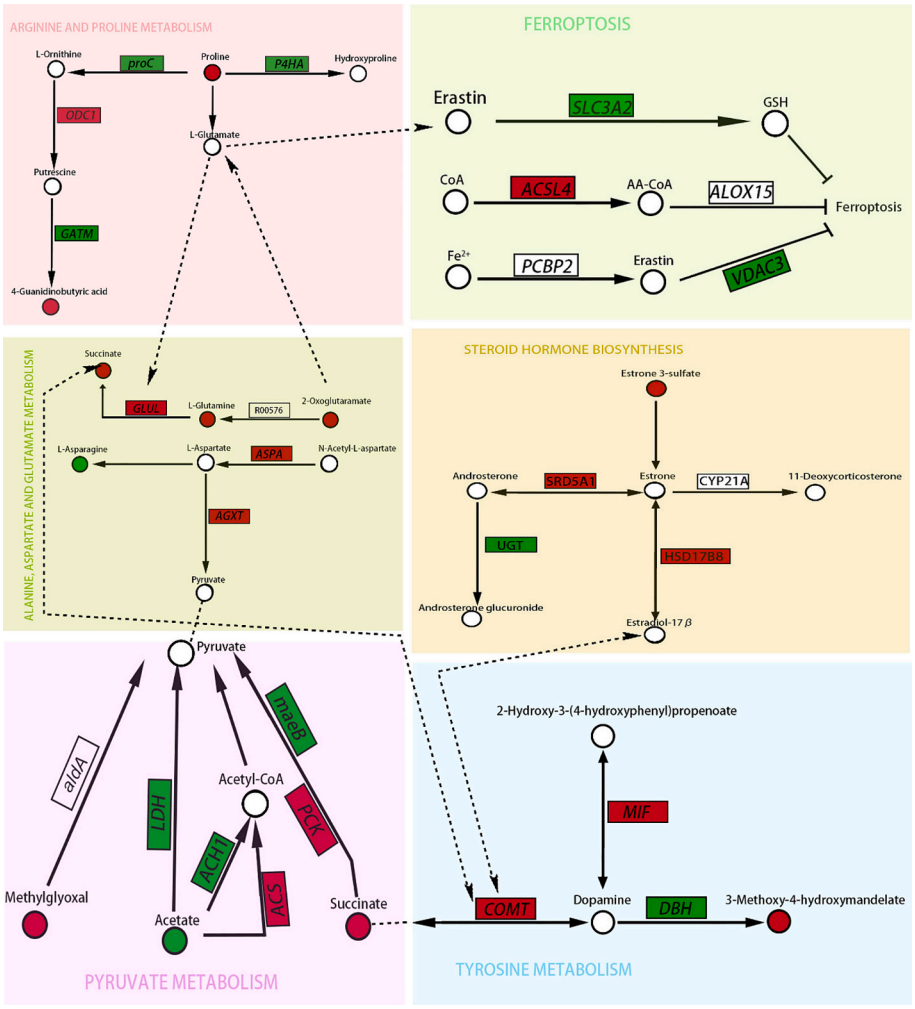

Fig. 7. Metabolic and transcriptional integration network map among WT, *mc3r*$^{+/-}$, and *mc4r*$^{+/-}$ in the liver.
The circles represent metabolites and the boxes represent genes. The significantly altered genes and metabolites in *mc3r*$^{+/-}$ and *mc4r*$^{+/-}$ are labeled red (upregulated) or green (downregulated) compared to WT. White circles and boxes indicate no difference. Ornithine decarboxylase (*ODC1*); Prolyl 4-hydroxylase (*P4HA*); Glycine amidinotransferase (*GATM*); Glutamine synthetase (*GLUL*); Aspartoacylase (*ASPA*); Alanine-glyoxylate transaminase (*AGXT*); Lactate dehydrogenase (*LDH*); Acetyl-CoA hydrolase (*ACH1*); Acetyl-COA Synthetase (*ACS*); Phosphoenolpyruvate carboxykinase (*PCK*); Malate dehydrogenase (*maeB*); Lactaldehyde dehydrogenase (*aldA*); Catechol *O*-methyltransferase (*COMT*); Macrophage migration inhibitory factor (*MIF*); Dopamine beta-monooxygenase (*DBH*); 17beta-estradiol 17-dehydrogenase (*HSD17B8*); 5 alpha-reductases (*SRD5A1*); Glucuronosyltransferase (*UGT*); Long-chain acyl-CoA synthetase (*ACSL4*); Solute carrier family 3, member 2 (*SLC3A2*); Voltage-dependent anion channel protein 3 (*VDAC3*); Poly(rC)-binding protein 2 (*PCBP2*).

progesterone synthesis (Liu et al., 2023a). Want5a, SMADs, IGF1R, and HGF are involved in folliculogenesis, luteogenesis, and ovulation. adipor1 affects ovarian steroid production, and genes like *MAD212*, *FOXM1*, and *MAPK1* indirectly influence ovarian development (Abedini et al., 2016; Gallelli et al., 2019; Li, 2015; Sirotkin, 2011; Wang et al., 2018; Chabrolle et al., 2007; Diaz et al., 2017; Ding et al., 2022; Ponza et al., 2011). In our study, KEGG enrichment analysis of WT vs. *mc3r*$^{+/-}$ indicated that 273 DEGs were enriched in 144 pathways and 13 pathways were significantly enriched ($p < 0.05$). In WT vs. *mc4r*$^{+/-}$, KEGG enrichment analysis showed that 516 DEGs were enriched in 155 pathways and 14 pathways were significantly enriched ($p < 0.05$). In *mc3r*$^{+/-}$ vs. *mc4r*$^{+/-}$, KEGG enrichment analysis revealed that 469 DEGs were enriched in 147 pathways and no pathway was significantly enriched ($p < 0.05$). In addition, we found DEGs enriched in some pathways related to ovarian growth and development.

Antioxidant gene GSR plays a vital role in maintaining oocyte competence (Katz-Jaffe et al., 2020; Yeh et al., 2005), while CALM1 and sGnRH induce follicular growth and ovarian maturation. MCM5 and PARP1 promote granulosa cell proliferation, and NME3 and PTPN11 are crucial for oocyte maturation and embryo development. FGF10 decreases estradiol secretion, affecting follicular development (Ngernsoungnern et al., 2008; Ngernsoungnern et al., 2009; Warma et al., 2021; Dang et al., 2018; Zhang et al., 2023; Desvignes et al., 2011; Idrees et al., 2019; Gasperin et al., 2012). Our findings suggested that the upregulation or downregulation of these genes in *mc3r*$^{+/-}$ and *mc4r*$^{+/-}$ compared to WT, indicating that Mc3r and Mc4r may influence ovarian development, follicle formation, and oocyte maturation in fish.

The HPG axis is essential for regulating the reproductive endocrine system in vertebrates (Maharajan et al., 2020; Park et al., 2016). To investigate the effect of Mc3r and Mc4r on reproductive processes, we examined key HPG axis genes in WT *mc3r*$^{+/-}$, and *mc4r*$^{+/-}$ RCC. Our results showed that these genes were down-regulated in mutant fish compared with WT fish, consistent with previous studies (Chai et al., 2006; Jiang et al., 2017; Limone et al., 1997). The KISS and GPR54 are crucial for HPG axis function and reproduction (Greives et al., 2007; Seminara et al., 2003; Imamura et al., 2017; Singh et al., 2021), while LHβ, FSHβ, LHR, FSHR, and GnRH, are vital for follicle development (Ni et al., 2007; Ramakrishnappa et al., 2005). CYP19A1A, expressed mainly in the ovary, regulates ovarian differentiation (Guiguen et al., 2010; Patil and Gunasekera, 2008; Su et al., 2023). Prolactin affects

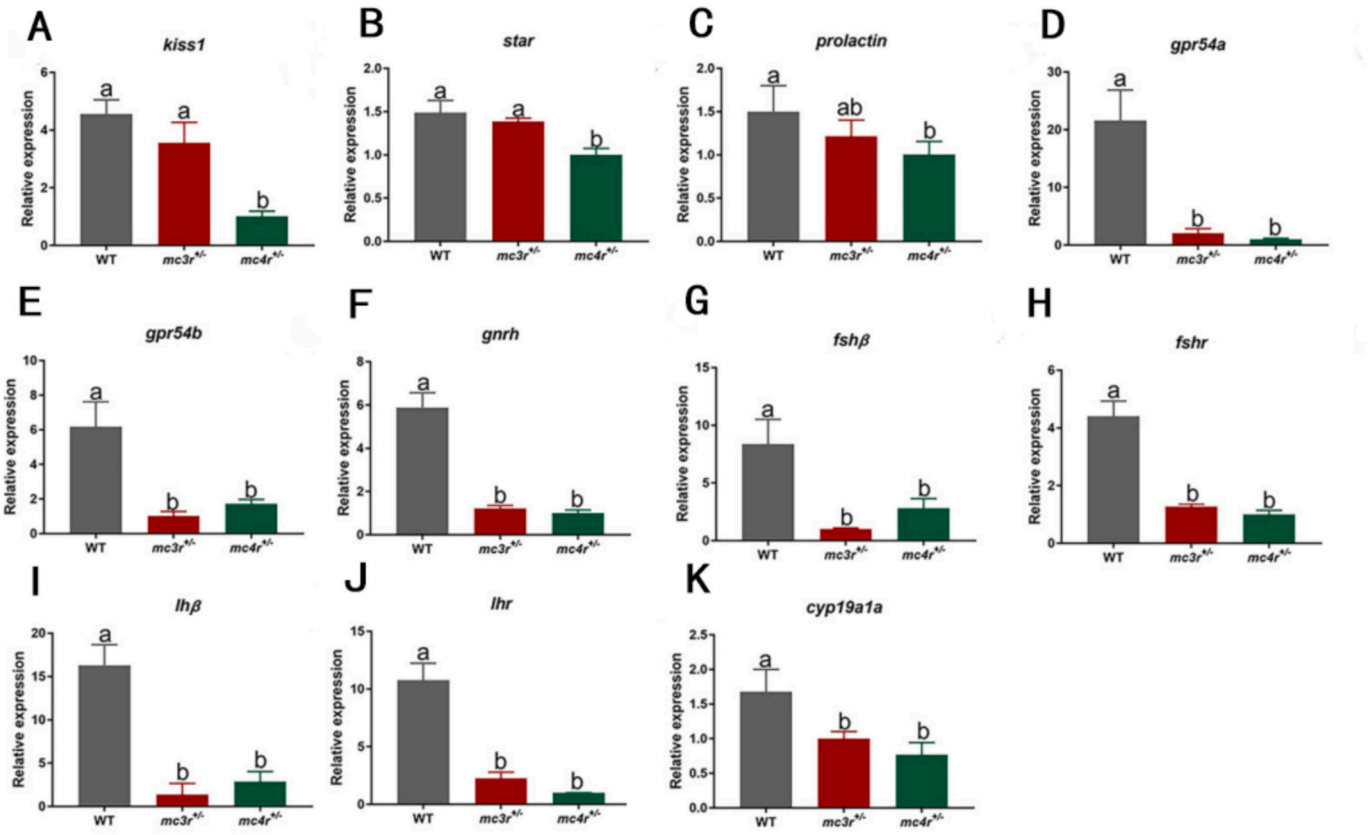

Fig. 8. Expression of key genes related to reproduction in WT, *mc3r*$^{+/-}$, and *mc4r*$^{+/-}$.
Expression of *kiss1* (A), *star* (B), *prolactin* (C), *gpr54a* (D), *gpr54b* (E), *gnrh* (F), *fshβ* (G), *fshr* (H), *lhβ* (I), *lhr* (J) and *cyp19a1a* (K) in WT, *mc3r*$^{+/-}$, and *mc4r*$^{+/-}$. kisspeptin-1 (*kiss1*); steroidogenic acute regulatory protein (*star*)G protein-coupled receptor a (*gpr54a*); G protein-coupled receptor b (*gpr54b*); gonadotropin-releasing hormone (*gnrh*); follicle-stimulating hormone beta (*fshβ*); follicle-stimulating hormone receptor (*fshr*); luteinizing hormone beta (*lhβ*); luteinizing hormone receptor (*lhr*); cytochrome P450 19A1 (*cyp19a1a*). Different letters indicated significant differences ($p < 0.05$). Data are shown as the mean ± SEM ($n = 3$).

testicular, ovarian, and uterine functions (Bachelot and Binart, 2007; Whittington and Wilson, 2013), and STAR is involved in steroidogenesis and gonad maturation (Nunez and Evans, 2007; Rathor et al., 2017; Sreenivasulu et al., 2009). Taken together, Mc3r and Mc4r might regulate ovarian development and reproduction by modulating hormone secretion via the HPG axis.

The development of the ovary is essential for fish reproduction (Chen et al., 2019). We observed a loss of contact between the follicular cell layer and the zona radiata in *mc3r*$^{+/-}$ and *mc4r*$^{+/-}$ RCC compared with the WT (Fig. 2), which further illustrated that the mutations in *mc3r* and *mc4r* influenced the development of oocytes. Remarkably, the above phenomenon described in the oocyte of *mc4r*$^{+/-}$ fish was more common than in *mc3r*$^{+/-}$ fish (Fig. 2B1, C1) (Table 1), which coincided with the results of ISH.

Growth performance and reproduction ability are key indicators in fish aquaculture. Both Mc3r and Mc4r play crucial roles in the growth and lipid accumulation of RCC (Huang et al., 2024). To explore how Mc3r and Mc4r regulate energy balance and reproduction, we performed metabolomic analyses on WT and mutant fish. We found that DMs were enriched in amino acid, lipid, and carbohydrate metabolism (Fig. 3A-C), consistent with our previous study in RCC (Huang et al., 2024). These metabolic pathways are crucial for physiological processes (Park et al., 2015), and the observed changes in DMs suggest that *mc3r* and *mc4r* mutations impact energy balance.

Our integrated transcriptome and metabolome analysis revealed that DEGs and DMs were enriched in pathways like arginine and proline metabolism, alanine, aspartate and glutamate metabolism, pyruvate metabolism, tyrosine metabolism, ferroptosis, and steroid hormone biosynthesis (Fig. 7). Key genes and metabolites involved in lipid accumulation and insulin resistance were identified, including proline, ornithine decarboxylase (ODC1), glycine amidinotransferase (GATM), and glutamine synthetase (GLUL). Up-regulation of succinate in alanine, aspartate, glutamate, and pyruvate metabolism can affect tyrosine metabolism and steroid hormone biosynthesis, impacting reproductive processes (Chaube and Joy, 2011).

We also found changes in steroid hormone biosynthesis, with up-regulated 17beta-estradiol 17-dehydrogenase (HSD17B8) and 5 alpha-reductases (SRD5A1), and down-regulated glucuronosyltransferase (UGT). These changes are linked to ovarian development and reproductive regulation (Liu et al., 2014; Kayampilly et al., 2010; Becedas et al., 1998). Ferroptosis-related metabolites like long-chain acyl-CoA synthetase (ACSL4), and changes in solute carrier family 3, member 2 (SLC3A2) and voltage-dependent anion channel protein 3 (VDAC3) were also noted, influencing ovarian health and fertility (Wang et al., 2024; Lee-Gyun and Park, 2017; Zinghirino et al., 2021). Our results suggest that Mc3r and Mc4r not only affect lipid accumulation and growth but also play a role in reproductive regulation, particularly ovarian development in fish.

5. Conclusion

In the study, we explored the role of Mc3r and Mc4r in regulating ovarian development via metabolomic sequencing, integrated analysis of the transcriptome and the metabolome, qRT-PCR, ISH, and HE. The localization of *mc3r* and *mc4r* mRNAs were detected in the pituitary gland and ovary, suggesting that *mc3r* and *mc4r* might be involved in regulating reproduction and ovarian development. Furthermore, DEGs were enriched in pathways, which were associated with reproduction

and ovarian development. The expression of key genes related to reproduction on the HPG axis was lower in *mc3r*$^{+/-}$ and *mc4r*$^{+/-}$ than in WT. Thus, Mc3r and Mc4r might have important roles in regulating the reproductive ability of female RCC. This study provides new insights into the molecular mechanisms by which Mc3r and Mc4r regulate ovarian development and offers a theoretical basis for enhancing reproductive strategies in teleost fish.

CRediT authorship contribution statement

Faxian Yu: Validation, Formal analysis. **Lu Huang:** Writing – original draft, Validation, Formal analysis, Data curation, Conceptualization. **Xinxin Yu:** Validation, Formal analysis. **Shuxin Zhang:** Validation. **Shengnan Li:** Validation. **Rong Zhou:** Formal analysis. **Wenjing Tao:** Writing – review & editing. **Lanying Yang:** Writing – review & editing. **Min Tao:** Writing – review & editing, Supervision, Funding acquisition, Conceptualization. **Qizhi Liu:** Writing – review & editing, Supervision. **Shaojun Liu:** Writing – review & editing, Supervision, Conceptualization.

Declaration of competing interest

The authors declare that they have no known competing financial interests or personal relationships that could have appeared to influence the work reported in this paper.

Acknowledgments

This research was supported by the National Natural Science Foundation of China (Grant No. 32293253, 32293252), the Hunan Province Science and Technology Innovation Platform and Talent Program Leading Talent (Grant No. 2023RC1053), the Postgraduate Science Research Innovation Project of Hunan Province (Grant No. CX20230523), the Earmarked Fund for China Agriculture Research System (Grant No. CARS-45), 111 Project (D20007).

Appendix A. Supplementary data

Supplementary data to this article can be found online at https://doi.org/10.1016/j.aquaculture.2025.742243.

Data availability

The datasets presented in this study can be found in online repositories. The raw reads were submitted to NCBI under accession PRJNA1107086.

References

Abedini, A., Zamberlam, G., Lapointe, E., Tourigny, C., Boyer, A., Paquet, M., Hayashi, K., Honda, H., Kikuchi, A., Price, C., 2016. WNT5a is required for normal ovarian follicle development and antagonizes gonadotropin responsiveness in granulosa cells by suppressing canonical WNT signaling. FASEB J. 30 (4), 1534.

Aldhoon Hainerová, I., Zamrazilová, H., Sedláčková, D., Hainer, V., 2011. Hypogonadotropic hypogonadism in a homozygous MC4R mutation carrier and the effect of sibutramine treatment on body weight and obesity-related health risks. Obes. Facts 4 (4), 324–328.

Aspiras, A.C., Rohner, N., Martineau, B., Borowsky, R.L., Tabin, C.J., 2015. Melanocortin 4 receptor mutations contribute to the adaptation of cavefish to nutrient-poor conditions. Proc. Natl. Acad. Sci. 112 (31), 9668–9673.

Bachelot, A., Binart, N., 2007. Reproductive role of prolactin. Reproduction 133 (2), 361–369.

Balthasar, N., Dalgaard, L.T., Lee, C.E., Yu, J., Funahashi, H., Williams, T., Ferreira, M., Tang, V., McGovern, R.A., Kenny, C.D., 2005. Divergence of melanocortin pathways in the control of food intake and energy expenditure. Cell 123 (3), 493–505.

Batarfi, A.A., Filimban, N., Bajouh, O.S., Dallol, A., Chaudhary, A.G., Bakhashab, S., 2019. MC4R variants rs12970134 and rs17782313 are associated with obese polycystic ovary syndrome patients in the Western region of Saudi Arabia. BMC Med. Genet. 20, 1–7.

Becedas, L., Lundgren, B., Pierre, J.W.D., 1998. Characterization of the UDP-glucuronosyltransferase isoenzyme expressed in rat ovary and its regulation by gonadotropins. Biochem. J. 332 (1), 51–55.

Bedenbaugh, M.N., Sweet, S., Mendoza-Romero, H., Brener, S., Hawkins, S., Yu, G., Zimmermann, J., Sweeney, P., Cone, R., Simerly, R., 2023. 28 Melanocortin 3 receptor in neural circuits linking metabolic state with reproduction and growth. J. Anim. Sci. 101 (Supplement_3), 231–232.

Chabrolle, C., Tosca, L., Crochet, S., Tesseraud, S., Dupont, J., 2007. Expression of adiponectin and its receptors (AdipoR1 and AdipoR2) in chicken ovary: potential role in ovarian steroidogenesis. Domest. Anim. Endocrinol. 33 (4), 480–487.

Chai, B., Li, J.-Y., Zhang, W., Newman, E., Ammori, J., Mulholland, M.W., 2006. Melanocortin-4 receptor-mediated inhibition of apoptosis in immortalized hypothalamic neurons via mitogen-activated protein kinase. Peptides 27 (11), 2846–2857.

Chaube, R., Joy, K.P., 2011. Estradiol-17β modulates dose-dependently hypothalamic tyrosine hydroxylase activity inhibited by α-methylparatyrosine in the catfish Heteropneustes fossilis. Endocrine 40, 394–399.

Chen, A.S., Marsh, D.J., Trumbauer, M.E., Frazier, E.G., Guan, X.M., Yu, H., Van der Ploeg, L.H., 2000. Inactivation of the mouse melanocortin-3 receptor results in increased fat mass and reduced lean body mass. Nat. Genet. 26 (1), 97–102.

Chen, H., Feng, W., Chen, K., Qiu, X., Xu, H., Mao, G., Zhao, T., Ding, Y., Wu, X., 2019. Transcriptomic analysis reveals potential mechanisms of toxicity in a combined exposure to dibutyl phthalate and diisobutyl phthalate in zebrafish (*Danio rerio*) ovary. Aquat. Toxicol. 216, 105290.

Cortés, R., Navarro, S., Agulleiro, M.J., Guillot, R., García-Herranz, V., Sánchez, E., Cerdá-Reverter, J.M., 2014. Evolution of the melanocortin system. Gen. Comp. Endocrinol. 209, 3–10.

Dang, Y., Wang, X., Hao, Y., Zhang, X., Zhao, S., Ma, J., Qin, Y., Chen, Z.J., 2018. MicroRNA-379-5p is associate with biochemical premature ovarian insufficiency through PARP1 and XRCC6. Cell Death Dis. 9 (2041-4889 (Electronic)), 106.

De Souza, F.S., Bumaschny, V.F., Low, M.J., Rubinstein, M., 2005. Subfunctionalization of expression and peptide domains following the ancient duplication of the proopiomelanocortin gene in teleost fishes. Mol. Biol. Evol. 22 (12), 2417–2427.

Desvignes, T., Fauvel, C., Bobe, J., 2011. The nme gene family in zebrafish oogenesis and early development. Naunyn Schmiedeberg's Arch. Pharmacol. 384 (4), 439–449.

Diaz, F.A., Foster, B.A., Hardin, P.T., Gutierrez, E.J., Bondioli, K.R., 2017. 131 Effect of prolonged progesterone exposure of beef cows on the expression of oocyte developmental competence-associated genes. Reprod. Fertil. Dev. 29 (1), 174.

Ding, C.Y., Lu, J.F., Li, J.C., Hu, X.J., Liu, Z.X., Su, H., Li, H., Huang, B.X., 2022. RNA-methyltransferase Nsun5 controls the maternal-to-zygotic transition by regulating maternal mRNA stability. Clin. Transl. Med. 12 (12).

Dores, R.M., Lecaude, S., 2005. Trends in the evolution of the proopiomelanocortin gene. Gen. Comp. Endocrinol. 142 (1–2), 81–93.

Doulla, M., McIntyre, A.D., Hegele, R.A., Gallego, P.H., 2014. A novel mutation associated with childhood-onset obesity: a case report. Paediatr. Child Health 19 (10), 515–518.

Du, Y.X., Ma, K.Y., Qiu, G.F., 2015. Discovery of the genes in putative GnRH signaling pathway with focus on characterization of GnRH- like receptor transcripts in the brain and ovary of the oriental river prawn. Aquaculture 442, 1–11.

Du, Y.Y., Yao, M.X., Yu, H.X., Mo, H.L., Yang, Q.Y., Yu, J.J., Wang, L.X., Zhou, J.S., Li, Y., 2023. Molecular cloning, tissue distribution, and pharmacologic function of melanocortin-3 receptor in common carp (*Cyprinus carpio*). Gen. Comp. Endocrinol. 330, 114149.

Duckett, K., Williamson, A., Kincaid, J.W.R., Rainbow, K., Corbin, L.J., Martin, H.C., Eberhardt, R.Y., Huang, Q.Q., Hurles, M.E., He, W., Brauner, R., Delaney, A., Dunkel, L., Grinspon, R.P., Hall, J.E., Hirschhorn, J.N., Howard, S.R., Latronico, A. C., Jorge, A.A.L., McElreavey, K., Mericq, V., Merino, P.M., Palmert, M.R., Plummer, L., Rey, R.A., Rezende, R.C., Seminara, S.B., Salnikov, K., Banerjee, I., Lam, B.Y.H., Perry, J.R.B., Timpson, N.J., Clayton, P., Chan, Y.M., Ong, K.K., O'Rahilly, S., 2023. Prevalence of deleterious variants in MC3R in patients with constitutional delay of growth and puberty. J. Clin. Endocrinol. Metab. 108 (12), E1570–E1577.

Dupont, J., Reverchon, M., Cloix, L., Froment, P., Ramé, C., 2012. Involvement of adipokines, AMPK, PI3K and the PPAR signaling pathways in ovarian follicle development and cancer. Int. J. Dev. Biol. 56 (10–12), 959–967.

Edmonds, J.W., Prasain, J.K., Dorand, D., Yang, Y.F., Hoang, H.D., Vibbert, J., Kubagawa, H.M., Miller, M.A., 2010. Insulin/FOXO signaling regulates ovarian prostaglandins critical for reproduction. Dev. Cell 19 (6), 858–871.

Gallelli, M.F., Bianchi, C., Lombardo, D., Rey, F., Rodriguez, F.M., Castillo, V.A., Miragaya, M., 2019. Leptin and IGF1 receptors in alpaca (*Vicugna pacos)* ovaries. Anim. Reprod. Sci. 200, 96–104.

Gantz, I., Fong, T.M., 2003. The melanocortin system. Am. J. Physiol. Endocrinol. Metab. 284 (3), E468–E474.

Gasperin, B.G., Ferreira, R., Rovani, M.T., Santos, J.T., Buratini, J., Price, C.A., Gonçalves, P.B.D., 2012. FGF10 inhibits dominant follicle growth and estradiol secretion in cattle. Reproduction 143 (6), 815–823.

Girardet, Clemence, Marks, Daniel L., Butler, Andrew A., 2018. Melanocortin-3 receptors expressed on agouti-related peptide neurons inhibit feeding behavior in female mice. Obesity (Silver Spring) 26 (12), 1849–1855.

Golyszny, M., Obuchowicz, E., Zielinski, M., 2022. Neuropeptides as regulators of the hypothalamus-pituitary-gonadal (HPG) axis activity and their putative roles in stress-induced fertility disorders. Neuropeptides 91, 102216.

Gothilf, Y., Muñoz-Cueto, J.A., Sagrillo, C.A., Selmanoff, M., Chen, T.T., Kah, O., Elizur, A., Zohar, Y., 1996. Three forms of gonadotropin-releasing hormone in a perciform fish (*Sparus aurata*): complementary deoxyribonucleic acid characterization and brain localization. Biol. Reprod. 55 (3), 636–645.

Greenstein, D., 2005. Control of oocyte meiotic maturation and fertilization. WormBook 28, 1–12.
Greives, T.J., Mason, A.O., Scotti, M.A.L., Levine, J., Ketterson, E.D., Kriegsfeld, L.J., Demas, G.E., 2007. Environmental control of kisspeptin: implications for seasonal reproduction. Endocrinology 148 (3), 1158–1166.
Guiguen, Y., Fostier, A., Piferrer, F., Chang, C.F., 2010. Ovarian aromatase and estrogens: a pivotal role for gonadal sex differentiation and sex change in fish. Gen. Comp. Endocrinol. 165 (3), 352–366.
Guzmán, J.M., Rubio, M., Ortiz-Delgado, J.B., Klenke, U., Kight, K., Cross, I., Sánchez-Ramos, I., Riaza, A., Rebordinos, L., Sarasquete, C., Zohar, Y., Mañanós, E.L., 2009. Comparative gene expression of gonadotropins (FSH and LH) and peptide levels of gonadotropin-releasing hormones (GnRHs) in the pituitary of wild and cultured Senegalese sole (*Solea senegalensis*) broodstocks. Comp. Biochem. Physiol. A Mol. Integr. Physiol. 153 (3), 266–277.
Herbison, A.E., 2018. The gonadotropin-releasing hormone pulse generator. Endocrinology 159 (11), 3723–3736.
Huang, L., Hu, H., Tao, M., Wang, Q.B., Li, T., Yang, X.Q., Fan, S.Y., Zhao, R.R., Wang, S., Liu, S.J., 2021. Elevated expression of *inhibin* α gene in sterile allotriploid crucian carp. Gen. Comp. Endocrinol. 312, 113856.
Huang, L., Deng, X., Yang, X.Q., Tang, Z., Fan, S.Y., Zhou, Z.F., Tao, M., Liu, S.J., 2024. Cloning, distribution, and effects of growth regulation of MC3R and MC4R in red crucian carp (*Carassius auratus* red var.). Front. Endocrinol. 14, 1310000.
Hussein, M.R., 2005. Apoptosis in the ovary: molecular mechanisms. Hum. Reprod. Update 11 (2), 162–178.
Huszar, D., Lynch, C.A., Fairchild-Huntress, V., Dunmore, J.H., Fang, Q., Berkemeier, L. R., Gu, W., Kesterson, R.A., Boston, B.A., Cone, R.D., Smith, F.J., Campfield, L.A., Burn, P., Lee, F., 1997. Targeted disruption of the Melanocortin-4 receptor results in obesity in mice. Cell 88 (1), 131–141.
Idrees, M., Xu, L.G., Song, S.H., Joo, M.D., Lee, K.L., Muhammad, T., El Sheikh, M., Sidrat, T., Kong, I.K., 2019. PTPN11 (SHP2) is indispensable for growth factors and cytokine signal transduction during bovine oocyte maturation and blastocyst development. Cells 8 (10), 1272.
Imamura, S., Hur, S.P., Takeuchi, Y., Bouchekioua, S., Takemura, A., 2017. Molecular cloning of kisspeptin receptor genes (gpr54-1 and gpr54-2) and their expression profiles in the brain of a tropical damselfish during different gonadal stages. Comp. Biochem. Physiol. A-Mol. Integr. Physiol. 203, 9–16.
Ji, R.L., Huang, L., Wang, Y., Liu, T., Fan, S.Y., Tao, M., Tao, Y.X., 2021. Topmouth culter melanocortin-3 receptor: regulation by two isoforms of melanocortin-2 receptor accessory protein 2. Endocr. Connect. 10 (11), 1489–1501.
Jiang, D.N., Li, J.T., Tao, Y.X., Chen, H.P., Deng, S.P., Zhu, C.H., Li, G.L., 2017. Effects of melanocortin-4 receptor agonists and antagonists on expression of genes related to reproduction in spotted scat, *Scatophagus argus*. J. Comp. Physiol. B-Biochem. Syst. Environ. Physiol. 187 (4), 603–612.
Josefsberg Ben-Yehoshua, L., Lewellyn, A.L., Thomas, P., Maller, J.L., 2007. The role of Xenopus membrane progesterone receptor β in mediating the effect of progesterone on oocyte maturation. Mol. Endocrinol. 21 (3), 664–673.
Katz-Jaffe, M.G., Lane, S.L., Parks, J.C., McCallie, B.R., Makloski, R., Schoolcraft, W.B., 2020. Antioxidant intervention attenuates aging-related changes in the murine ovary and oocyte. Life 10 (11).
Kayampilly, P.P., Wanamaker, B.L., Stewart, J.A., Wagner, C.L., Menon, K.M.J., 2010. Stimulatory effect of insulin on 5α-reductase type 1 (SRD5A1) expression through an Akt-dependent pathway in ovarian granulosa cells. Endocrinology 151 (10), 5030–5037.
Knobil, E., 1990. The GnRH pulse generator. Am. J. Obstet. Gynecol. 163 (5), 1721–1727.
Lam, B.Y.H., Williamson, A., Finer, S., Day, F.R., Tadross, J.A., Soares, A.G., Wade, K., Sweeney, P., Bedenbaugh, M.N., Porter, D.T., Melvin, A., Ellacott, K.L.J., Lippert, R. N., Buller, S., Rosmaninho-Salgado, J., Dowsett, G.K.C., Ridley, K.E., Xu, Z., Cimino, I., Rimmington, D., Rainbow, K., Duckett, K., Holmqvist, S., Khan, A., Dai, X., Bochukova, E.G., Trembath, R.C., Martin, H.C., Coll, A.P., Rowitch, D.H., Wareham, N.J., van Heel, D.A., Timpson, N., Simerly, R.B., Ong, K.K., Cone, R.D., Langenberg, C., Perry, J.R.B., Yeo, G.S., O'Rahilly, S., 2021. MC3R links nutritional state to childhood growth and the timing of puberty. Nature 599 (7885), 436–441.
Lampert, K.P., Schmidt, C., Fischer, P., Volff, J.N., Hoffmann, C., Muck, J., Lohse, M.J., Ryan, M.J., Schartl, M., 2010. Determination of onset of sexual maturation and mating behavior by Melanocortin receptor 4 polymorphisms. Curr. Biol. 20 (19), 1729–1734.
Lee-Gyun, O., Park, C.-E., 2017. The expression of solute carrier family members genes in mouse ovarian developments. Korean J. Clin. Lab. Sci. 49 (1), 40–47.
Li, Q., 2015. Inhibitory SMADs: potential regulators of ovarian Function1. Biol. Reprod. 92 (2), 51–56, 50.
Limone, P., Calvelli, P., Altare, F., Ajmone-Catt, P., Lima, T., Molinatti, G.M., 1997. Evidence for an interaction between α-MSH and opioids in the regulation of gonadotropin secretion in man. J. Endocrinol. Investig. 20, 207–210.
Lin, C.Y., Chen, C.Y., Yu, C.H., Yu, I.S., Lin, S.R., Wu, J.T., Lin, Y.H., Kuo, P.L., Wu, J.C., Lin, S.W., 2016. Human X-linked intellectual disability factor CUL4B is required for post-meiotic sperm development and male fertility. Sci. Rep. 6 (1), 20227.
Liu, J.G., Zhang, Z.F., Ma, X.S., Liang, S.S., Yang, D.D., 2014. Characteristics of 17β-hydroxysteroid dehydrogenase 8 and its potential role in gonad of Zhikong scallop. J. Steroid Biochem. Mol. Biol. 141, 77–86.
Liu, R.Q., Kinoshita, M., Adolfi, M.C., Schart, M., 2019. Analysis of the role of the Mc4r system in development, growth, and puberty of Medaka. Front. Endocrinol. 10, 442453.
Liu, R., Du, K., Ormanns, J., Adolfi, M.C., Schartl, M., 2020. Melanocortin 4 receptor signaling and puberty onset regulation in Xiphophorus swordtails. Gen. Comp. Endocrinol. 295, 113521.
Liu, Z.B., Zhang, J.B., Li, S.P., Yu, W.J., Pei, N., Jia, H.T., Li, Z., Lv, W.F., Wang, J., Kim, N.H., Yuan, B., Jiang, H., 2023a. ID3 regulates progesterone synthesis in bovine cumulus cells through modulation of mitochondrial function. Theriogenology 209, 141–150.
Liu, F., Zhang, X.L., Wei, X.K., Li, Y., Liu, W., Gan, G.C., Xiao, L.L., Wang, X.Y., Luo, H., 2023b. Gonadal transcriptome analysis of paradise fish *Macropodus opercularis* to reveal sex-related genes. Comp. Biochem. Physiol. D-Genomics Proteomics 48, 101125.
Livak, K.J., Schmittgen, T.D., 2001. Analysis of relative gene expression data using real-time quantitative PCR and the $2^{-\Delta\Delta CT}$ method. Methods 25 (4), 402–408.
Maharajan, K., Muthulakshmi, S., Karthik, C., Nataraj, B., Nambirajan, K., Hemalatha, D., Jiji, S., Kadirvelu, K., Liu, K.-C., Ramesh, M., 2020. Pyriproxyfen induced impairment of reproductive endocrine homeostasis and gonadal histopathology in zebrafish (Danio rerio) by altered expression of hypothalamus-pituitary-gonadal (HPG) axis genes. Sci. Total Environ. 735, 139496.
Manfredi-Lozano, M., Roa, J., Ruiz-Pino, F., Piet, R., Garcia-Galiano, D., Pineda, R., Zamora, A., Leon, S., Sanchez-Garrido, M.A., Romero-Ruiz, A., Dieguez, C., Vazquez, M.J., Herbison, A.E., Pinilla, L., Tena-Sempere, M., 2016. Defining a novel leptin-melanocortin-kisspeptin pathway involved in the metabolic control of puberty. Mol. Metab. 5 (10), 844–857.
Mantawy, E.M., Said, R.S., Abdel-Aziz, A.K., 2019. Mechanistic approach of the inhibitory effect of chrysin on inflammatory and apoptotic events implicated in radiation-induced premature ovarian failure: emphasis on TGF-β/MAPKs signaling pathway. Biomed. Pharmacother. 109, 293–303.
Martin, W.J., MacIntyre, D.E., 2004. Melanocortin receptors and erectile function. Eur. Urol. 45 (6), 706–713.
Navarro, S., Crespo, D., Schulz, R.W., Ge, W., Rotllant, J., Cerdá-Reverter, J.M., Rocha, A., 2022. Role of the Melanocortin system in gonadal steroidogenesis of zebrafish. Animals 12 (20).
Ngernsoungnern, A., Ngernsoungnern, P., Weerachatyanukul, W., Chavadej, J., Sobhon, P., Sretarugsa, P., 2008. The existence of gonadotropin-releasing hormone (GnRH) immunoreactivity in the ovary and the effects of GnRHs on the ovarian maturation in the black tiger shrimp. Aquaculture 279 (1–4), 197–203.
Ngernsoungnern, P., Ngernsoungnern, A., Dobhon, P., Sretarugsa, P., 2009. Gonadotropin-releasing hormone (GnRH) and a GnRH analog induce ovarian maturation in the giant freshwater prawn, *Macrobrachium rosenbergii*. Invertebr. Reprod. Dev. 53 (3), 125–135.
Ni, Y.D., Zhou, Y.C., Lu, L.Z., Grossmann, R., Zhao, R.Q., 2007. Developmental changes of FSH-R, LH-R, ER-β and GnRH-I expression in the ovary of prepubertal ducks (*Anas platyrhynchos*). Anim. Reprod. Sci. 100 (3–4), 318–328.
Nunez, B.S., Evans, A.N., 2007. Hormonal regulation of the steroidogenic acute regulatory protein (StAR) in gonadal tissues of the Atlantic croaker (*Micropogonias undulatus*). Gen. Comp. Endocrinol. 150 (3), 495–504.
Pandolfi, M., Lo Nostro, F.L., Shimizu, A., Pozzi, A.G., Meijide, F.J., Vazquez, G.R., Maggese, M.C., 2006. Identification of immunoreactive FSH and LH cells in the cichlid fish *Cichlasoma dimerus* during the ontogeny and sexual differentiation. Anat. Embryol. 211 (5), 355–365.
Park, S., Sadanala, K.C., Kim, E.K., 2015. A metabolomic approach to understanding the metabolic link between obesity and diabetes. Mol. Cell 38 (7), 587–596.
Park, J.W., Jin, Y.H., Oh, S.Y., Kwon, J.Y., 2016. Kisspeptin2 stimulates the HPG axis in immature Nile tilapia (*Oreochromis niloticus*). Comp. Biochem. Physiol. B-Biochem. Mol. Biol. 202, 31–38.
Patil, J.G., Gunasekera, R.M., 2008. Tissue and sexually dimorphic expression of ovarian and brain aromatase mRNA in the Japanese medaka (*Oryzias latipes*): implications for their preferential roles in ovarian and neural differentiation and development. Gen. Comp. Endocrinol. 158 (1), 131–137.
Ponza, P., Yocawibun, P., Sittikankaew, K., Hiransuchalert, R., Yamano, K., Klinbunga, S., 2011. Molecular cloning and expression analysis of the *Mitogen-activating protein kinase 1 (MAPK1)* gene and protein during ovarian development of the giant tiger shrimp *Penaeus monodon*. Mol. Reprod. Dev. 78 (5), 347–360.
Qiu, G.F., Ramachandra, R.K., Rexroad, C.E., Yao, J.B., 2008. Molecular characterization and expression profiles of cyclin B1, B2 and Cdc2 kinase during oogenesis and spermatogenesis in rainbow trout (*Oncorhynchus mykiss*). Anim. Reprod. Sci. 105 (3–4), 209–225.
Ramakrishnappa, N., Rajamahendran, R., Lin, Y.M., Leung, P.C.K., 2005. GnRH in non-hypothalamic reproductive tissues. Anim. Reprod. Sci. 88 (1–2), 95–113.
Rathor, P.K., Bhat, I.A., Rather, M.A., Gireesh-Babu, P., Kumar, K., Purayil, S.B.P., Sharma, R., 2017. Steroidogenic acute regulatory protein (StAR) gene expression construct: development, nanodelivery and effect on reproduction in air-breathing catfish, *Clarias batrachus*. Int. J. Biol. Macromol. 104, 1082–1090.
Sandrock, M., Schulz, A., Merkwitz, C., Schöneberg, T., Spanel-Borowski, K., Ricken, A., 2009. Reduction in corpora lutea number in obese melanocortin-4-receptor-deficient mice. Reprod. Biol. Endocrinol. 7 (1), 24.
Schjolden, J., Schiöth, H.B., Larhammar, D., Winberg, S., Larson, E.T., 2009. Melanocortin peptides affect the motivation to feed in rainbow trout (*Oncorhynchus mykiss*). Gen. Comp. Endocrinol. 160 (2), 134–138.
Seminara, S.B., Messager, S., Chatzidaki, E.E., Thresher, R.R., Acierno Jr., J.S., Shagoury, J.K., Bo-Abbas, Y., Kuohung, W., Schwinof, K.M., Hendrick, A.G., 2003. The GPR54 gene as a regulator of puberty. N. Engl. J. Med. 349 (17), 1614–1627.
Singh, A., Lal, B., Parhar, I.S., Millar, R.P., 2021. Seasonal expression and distribution of kisspeptin1 (kiss1) in the ovary and testis of freshwater catfish, Clarias batrachus: a putative role in steroidogenesis. Acta Histochem. 123 (6), 151766.
Sirotkin, A.V., 2011. Growth factors controlling ovarian functions. J. Cell. Physiol. 226 (9), 2222–2225.
Sreenivasulu, G., Sridevi, P., Sahoo, P.K., Swapna, I., Ge, W., Kirubagaran, R., Dutta-Gupta, A., Senthilkumaran, B., 2009. Cloning and expression of StAR during gonadal

cycle and hCG-induced oocyte maturation of air-breathing catfish, *Clarias gariepinus*. Comp. Biochem. Physiol. B-Biochem. Mol. Biol. 154 (1), 6–11.
Strauss, J.F., Modi, B., McAllister, J.M., 2014. Defects in ovarian steroid hormone biosynthesis. In: Ulloa-Aguirre, A., Conn, P.M. (Eds.), Cellular Endocrinology in Health and Disease. Academic Press, Boston, pp. 285–309.
Su, J.X., Yi, S.K., Gao, Z.X., Abbas, K., Zhou, X.Y., 2023. DNA methylation mediates gonadal development via regulating the expression levels of cyp19a1a in loach Misgurnus anguillicaudatus. Int. J. Biol. Macromol. 235, 123794.
Swanson, P., Dickey, J.T., Campbell, B., 2003. Biochemistry and physiology of fish gonadotropins. Fish Physiol. Biochem. 28, 53–59.
Tao, M., Ji, R.L., Huang, L., Fan, S.Y., Liu, T., Liu, S.J., Tao, Y.X., 2020. Regulation of Melanocortin-4 receptor pharmacology by two isoforms of Melanocortin receptor accessory protein 2 in Topmouth Culter (Culter alburnus). Front. Endocrinol. 11, 538.
Tilly, J., 1996. Apoptosis and ovarian function. Rev. Reprod. 1 (3), 162–172.
Volff, J.N., Selz, Y., Hoffmann, C., Froschauer, A., Schultheis, C., Schmidt, C., Zhou, Q.C., Bernhardt, W., Hanel, R., Böhne, A., Brunet, F., Ségurens, B., Couloux, A., Bernard-Samain, S., Barbe, V., Ozouf-Costaz, C., Galiana, D., Lohse, M.J., Schartl, M., 2013. Gene amplification and functional diversification of Melanocortin 4 receptor at an extremely polymorphic locus controlling sexual maturation in the Platyfish. Genetics 195 (4), 1337–1352.
Wang, D.H., Ren, J., Zhou, C.J., Han, Z., Wang, L., Liang, C.G., 2018. Supplementation with CTGF, SDF1, NGF, and HGF promotes ovine in vitro oocyte maturation and early embryo development. Domest. Anim. Endocrinol. 65, 38–48.
Wang, S., Li, X., Li, J., Wang, A., Li, F., Hu, H., Long, T., Pei, X., Li, H., Zhong, F., Zhu, F., 2024. Inhibition of cisplatin-induced Acsl4-mediated ferroptosis alleviated ovarian injury. Chem. Biol. Interact. 387, 11082.
Warma, A., Lussier, J.G., Ndiaye, K., 2021. Tribbles Pseudokinase 2 (TRIB2) regulates expression of binding partners in Bovine Granulosa cells. Int. J. Mol. Sci. 22 (4), 1533.
Watanobe, H., Schiöth, H.B., Wikberg, J.E.S., Suda, T., 1999. The melanocortin 4 receptor mediates leptin stimulation of luteinizing hormone and prolactin surges in steroid-primed ovariectomized rats. Biochem. Biophys. Res. Commun. 257 (3), 860–864.
Watanobe, H., Yoneda, M., Kakizaki, Y., Kohsaka, A., Suda, T., Schiöth, H.B., 2001. Further evidence for a significant participation of the melanocortin 4 receptor in the preovulatory prolactin surge in the rat. Brain Res. Bull. 54 (5), 521–525.
Whittington, C.M., Wilson, A.B., 2013. The role of prolactin in fish reproduction. Gen. Comp. Endocrinol. 191, 123–136.
Wu, L., Yu, H., Mo, H., Lan, X., Pan, C., Wang, L., Zhao, H., Zhou, J., Li, Y., 2022. Functional characterization of Melanocortin-3 receptor in a hibernating cavefish Onychostoma macrolepis. Animals 12 (1).
Yang, Q., Yang, X., Liu, J., Ren, W., Chen, Y., Shen, S., 2017. Effects of BPF on steroid hormone homeostasis and gene expression in the hypothalamic–pituitary–gonadal axis of zebrafish. Environ. Sci. Pollut. Res. 24, 21311–21322.
Yang, L.K., Zhang, Z.R., Wen, H.S., Tao, Y.X., 2019. Characterization of channel catfish (*Ictalurus punctatus*) melanocortin-3 receptor reveals a potential network in regulation of energy homeostasis. Gen. Comp. Endocrinol. 277, 90–103.
Yeh, J., Bowman, M.J., Browne, R.W., Chen, N., 2005. Reproductive aging results in a reconfigured ovarian antioxidant defense profile in rats. Fertil. Steril. 84, 1109–1113.
Yu, C., 2014. CRL4 complex regulates mammalian oocyte survival and reprogramming by activation of TET proteins. Science 344 (6183), 469.
Yu, H.X., Li, Y., Song, W.J., Wang, H., Mo, H.L., Liu, Q., Zhang, X.M., Jiang, Z.B., Wang, L.X., 2022. Functional characterization of melanocortin-3 receptor in rainbow trout (*Oncorhynchus mykiss*). Fish Physiol. Biochem. 48 (1), 241–252.
Zhang, Y., Kilroy, G.E., Henagan, T.M., Prpic-Uhing, V., Richards, W.G., Bannon, A.W., Mynatt, R.L., Gettys, T.W., 2005. Targeted deletion of melanocortin receptor subtypes 3 and 4, but not CART, alters nutrient partitioning and compromises behavioral and metabolic responses to leptin. FASEB J. 19 (11), 1482–1491.
Zhang, C., Forlano, P.M., Cone, R.D., 2012. AgRP and POMC neurons are hypophysiotropic and coordinately regulate multiple endocrine axes in a larval teleost. Cell Metab. 15 (2), 256–264.
Zhang, Y., Wen, H.S., Li, Y., Lyu, L.K., Zhang, Z.X., Wang, X.J., Li, J.S., Tao, Y.X., Qi, X., 2020. Melanocortin-4 receptor regulation of reproductive function in black rockfish (*Sebastes schlegelii*). Gene 741, 144541.
Zhang, Y., Wang, H.B., Zhu, Y., Hou, X.J., Li, X., Zhou, X.M., Ge, L.L., Xu, J., Su, Y.P., 2023. The novel peptide PFAP1 promotes primordial follicle activation by binding to MCM5. FASEB J. 37 (5).
Zheng, Y.R., Rajcsanyi, L.S., Peters, T., Dempfle, A., Wudy, S.A., Hebebrand, J., Hinney, A., 2023. Evaluation of the MC3R gene pertaining to body weight and height regulation and puberty development. Sci. Rep. 13 (1), 10419.
Zinghirino, F., Pappalardo, X.G., Messina, A., Nicosia, G., De Pinto, V., Guarino, F., 2021. VDAC genes expression and regulation in mammals. Front. Physiol. 12, 708695.